

Chapter 4

Results and Discussion

4.1 Background

In this Chapter results of the experiments carried out with agricultural based residues, such as wash waters from a potato wafer processing industry containing potato starch, molasses from the sugarcane industry and rice bran from rice polishing industry, as substrates for the production of lipopeptide type biosurfactant via fermentation technique utilizing the organism *B.subtilis* MTCC 2423 is discussed. The recovery and concentration of the biosurfactant using foam separation technique and its identification and characterization are also discussed.

A brief summary of lipopeptide biosurfactants produced using the microorganism *Bacillus subtilis* utilizing various agro based substrates is listed in Table 4.1. As detailed in Chapter 2, Literature Survey a number of agro substrates have been investigated for the production of biosurfactants using different microorganisms. It is rather surprising that the use of rice bran, that amount to huge quantity specifically in India and other Asian countries has not been explored for the production of biosurfactants.

Table 4.1: Lipopeptide type biosurfactant yields from agrowastes.

Bacillus subtilis strain	Agro waste	Biosurfactant type	Yield	Reference
ATCC 21332	Peat hydrolysate	Surfactin	0.14g/g sugar	Sheppard and Mulligan (1987)
MI 113	Okara waste	Surfactin	2.0 g/kg	Ohno et al. (1995)
ATCC 21332	Purified starch	Surfactin	0.154g/g starch	Fox and Bala (2000)
Bacillus subtilis	Potato process effluent	Lipopeptide	2.7 g/l	Noah et al. (2005)
B. subtilis ATCC 21332, B. subtilis LB5a	Cassava flour wastewater	Lipopeptide	2.2 g/l	Nitschke and Pastore (2006)

As per the data available from Government of India, Ministry of Agriculture, India ranks second in the world for rice production with 89.09 million tonnes for the year 2009-10. According to the survey of local rice mills, approximately 10-12 kg of rice bran and 55-60 kg of rice is generated per 100 kg of raw rice processed during polishing process in rice mill. The ratio of rice bran to that of rice ranges from 0.18 - 0.25, based on the above

ratio approximately 16.04 - 22.27 million tonnes of rice bran was produced in the year 2009-10.

Rice bran if processed within 24 hrs can be used for the extraction of rice bran oil for edible purpose. However, extraction of rice bran oil within 12-24 hr of rice bran production is not always feasible at local rice mills. Therefore, most of the rice bran is utilized only for cattle feed. Looking at huge production of rice bran and its easy availability, the utilization of rice bran as substrate for production of biosurfactant with *B.subtilis* MTCC 2423 was explored in this investigation.

Molasses, a byproduct of sugar manufacturing industry, has been used as a substrate for the production of biosurfactant – surfactin using *B.subtilis* MTCC 2423 (Makkar and Cameotra, 1997). Some investigators have used (Fox and Bala, 2000, Noah et al., 2005) potato starch for production of lipopeptide type biosurfactants using *B. subtilis* strain, the biosurfactant synthesized was identified to be “Surfactin”.

In this study starch containing waters of potato processing units was used as substrate for the biosurfactant production using *B. subtilis* MTCC2423 to develop standard operating procedure for fermentation. Subsequently this procedure was used to investigate the biosurfactant production using the other two substrates with some minor modifications as felt necessary during the course of investigation.

4.2 Potato starch as substrate for biosurfactant production

Three different sources of potato starch were utilized as the carbon source for the production of biosurfactant using *B.subtilis* MTCC 2423. The fermentation media M1 consisted of soluble starch 2% (w/v) procured from Hi media, media M2 was prepared from the starch containing wash liquid of potato chips prepared domestically and media M3 was a starch containing effluent generated during washing of potatoes from Jabson’s potato processing industry.

Fermentation experiments were carried out in an orbital shaking incubator at 30°C and 150 rpm for varying time intervals and production of the biosurfactant was monitored up to 72 hours. During the preliminary experiments different mineral salts KH_2PO_4 , Na_2HPO_4 , $(\text{NH}_4)_2\text{HPO}_4$, MgSO_4 , FeSO_4 , and CaCl_2 were added to the fermentation

media to optimize the biosurfactant yield by varying their content. After a series of experiments the optimized values were found to be 30mM KH_2PO_4 , 40mM, Na_2HPO_4 , 50 mM, $(\text{NH}_4)_2\text{HPO}_4$, 800 μM MgSO_4 , 4 μM FeSO_4 , and 7 μM CaCl_2 . Therefore, in all the subsequent experiments involving fermentation of potato starch the salt concentrations were maintained at the above listed values.

4.2.1 Drop collapse test

Screening of bacteria for its biosurfactant production capability is effectively and rapidly determined using a drop collapse test (Jain et al.,1991; Tugrul and Cansunar, 2005). The drop collapse test is a qualitative test that indicates the presence of surfactant even when its concentration in sample is low. This test was carried out for verification of the biosurfactant production ability of the *B.subtilis* MTCC 2423. The test was performed by utilizing cell free fermented broth. Two test samples were prepared, one with oil taken in a small well (2.5 ml) and a drop of cell free supernatant derived from fermentation put at the centre of the well. The second sample was prepared with same oil quantity in another well but a drop of distilled water was put at the centre of the well.

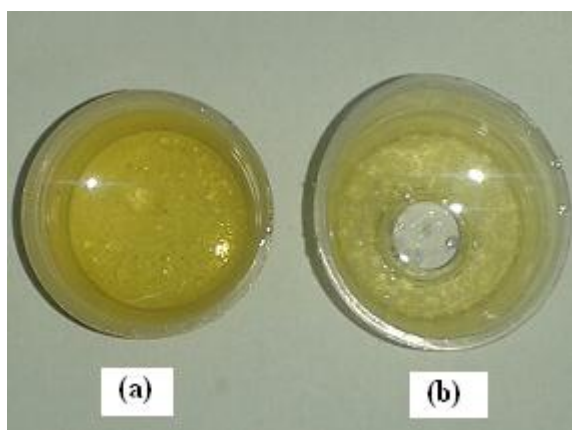


Fig. 4.1: Drop collapse test. (a) Drop of cell free supernatant on oil surface, (b) Drop of distilled water on oil surface

As observed in Figure 4.1, the drop of cell free supernatant derived from fermentation broth collapsed within few seconds while the drop of distilled water did not collapse. The behavior observed with the fermentation broth is attributed to the biosurfactant produced by fermentation that causes a reduction in the interfacial tension between the oily surface and water which helps in spreading the water drop over the oil and eventual solubilization of the drop. While the drop test was indicative of the presence of surfactant synthesized by fermentation of broth by *B.subtilis* MTCC 2423, the extent of surface

tension lowering and its correlation to the growth of the microorganism was investigated quantitatively to decide the time duration of fermentation for optimal production of biosurfactant.

4.2.2 Surface tension reduction with time

Screening of the biosurfactant producing microorganism is also carried out by monitoring the surface tension to estimate the surface activity. The decline in surface tension due to biosurfactant synthesis from potato starch media by fermentation using *B.subtilis* MTCC 2423 in the three media M1(Himedia starch), M2 (Potato processing effluent-Domestic) and M3(Potato processing effluent-Industrial) was measured at different time intervals. A plot of decline in surface tension with fermentation time is shown in Figure 4.2, where it is seen that in the initial 24 hours of fermentation there was a sharp decline in the surface tension from 70 mN/m to ~ 34 mN/m, thereafter the decline in surface tension was gradual and attained a value of 27 mN/m in 48 hours of fermentation time.

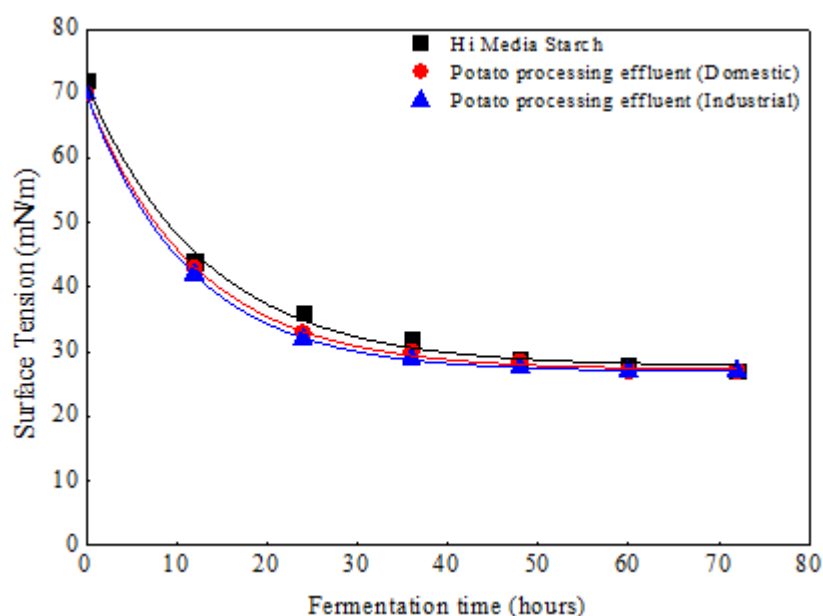


Fig. 4.2: Decline in surface tension with time of fermentation

The surface tension values remained constant till the end of the fermentation period of 72 hours. The surface tension values had a variation of around $\pm 3\%$ and all the experiments were done in triplicate. The nature of the surface tension – time plots was nearly similar for all the three media studied. The small difference observed in surface tension values observed for sample (M1) between 12 and 40 hours, in comparison with the other two samples, stems from the initial sugar content of the samples which was less

in (M1) compared with (M2) and (M3), thereby leading to increased synthesis of the surfactant. This led to increased lowering of the values of surface tension in (M2) and (M3). These results corroborate the findings of Fox and Bala (2000) who reported that higher initial soluble carbohydrate content of potato starch results in lower surface tension values.

The effect of starch concentration on biosurfactant production was investigated to validate the results observed in Fig. 4.2. Experiments were conducted by varying soluble starch content (Hi media) in the fermentation media in the range of 1.5 - 3% while maintaining the mineral salts and nutrient concentration constant at values reported earlier. Figure 4.3 shows the effect of initial starch content on the surface tension values at varying time intervals. Reduction in the surface tension was almost similar in the media having starch concentration of 2%, 2.5% and 3.0% (w/v). However, the reduction was marginally less in the medium containing 1.5% starch.

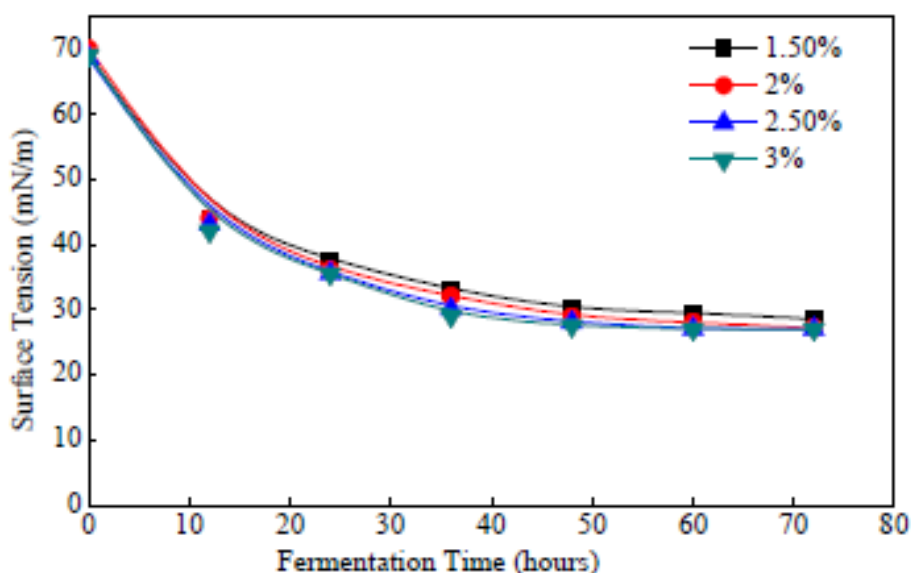


Fig.4.3: Effect of starch concentration on surface tension reduction

After 72 hours of fermentation, the lowest surface tension value recorded with 1.5% (w/v) starch media was 28.5 mN/m while, in the media containing 2%, 2.5% and 3.0% (w/v) starch the lowest value was 27 mN/m. These results indicate that that 1.5% (w/v) starch content was not the optimal substrate concentration with *B.subtilis* MTCC 2423 for biosurfactant production and the organism could use up higher initial starch content for the production that eventually resulted in greater reduction of surface tension of the medium.

4.2.3 Cell growth and carbohydrate utilization by *B.subtilis* MTCC 2423

The results obtained using potato starch as substrate reported in the previous section were quite encouraging and these experiments helped in establishing the operating procedures for (i) growth of *B. Subtilis* and (ii) the fermentation process using *B. Subtilis*. Attempts were not made to identify the bio surfactant since it is quite well established that fermentation of potato starch substrate using *B. Subtilis* results in production of surfactin (Fox and Bala, 2000). The next objective was to use molasses as well as rice bran as substrates using *B. Subtilis* to study the efficacy of biosurfactant production and also to isolate and identify the biosurfactant produced. The details are listed in the following sections.

As the first step the cell growth pattern of *B.subtilis* in the three substrates and effects of nutrients and carbohydrate consumption on growth of the microorganism was established and compared.

4.2.4 Growth of *Bacillus subtilis* using potato starch

Growth characteristics of *B.subtilis* MTCC 2423 using potato processing industry effluent as substrate is illustrated in Fig. 4.4. The curve resembles a typical bacterial population growth curve exhibiting all the four phases. The lag phase was ~ 6 hours; this

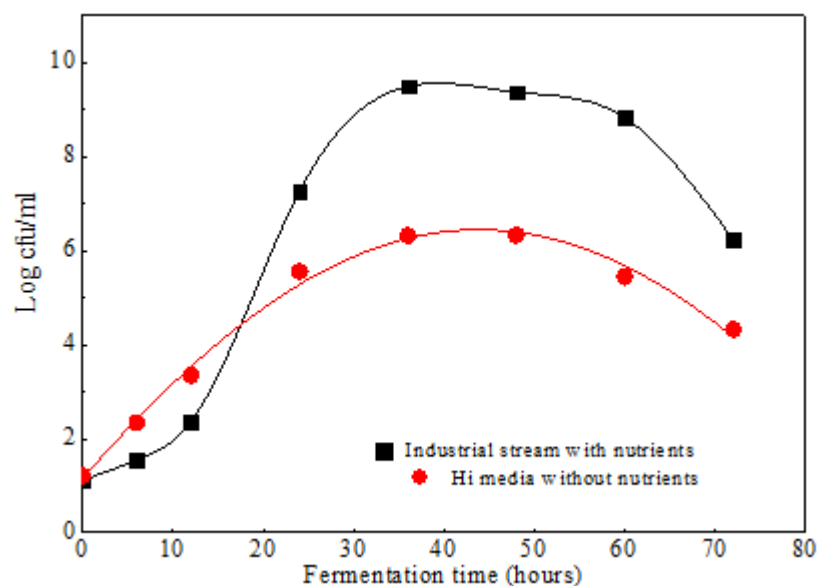


Fig.4.4: Effect of nutrients on growth for *B.subtilis*

was the time when the cells were adjusting to the new environment. The cells increased in size however there was no cell division which is evident from the approximately constant colony forming units (cfu) values. After 6 hours of fermentation there was

considerable increase in (cfu), which continued up to 36 hours. This was the log phase where under optimum conditions the cells reproduce at a uniform and rapid rate resulting in an exponential increase in their population.

Maximum bacterial growth of $\sim 10^{10}$ cfu/mL was observed at 36 hours during fermentation. Stationary growth phase started at 36 hours and continued upto 60 hours. The growth was maintained up to 60 hours and then there was decline in cfu, this corresponded with the death phase period wherein there was depletion of essential nutrients and an accumulation of the metabolic wastes in the medium. The growth curve of *B.subtilis* is closely associated with the carbohydrate availability during the course of fermentation.

The total sugar consumption during the bacterial growth shows a continuous decline indicating the consumption of sugar during fermentation as shown in Fig. 4.5. Initially a sharp reduction in the total sugar concentration is observed from 0 to 36 hours and thereafter the reduction slowed down considerably and became constant after 60 hours. This is attributed to higher nutrition requirement for cell growth and for production of extracellular products during exponential phase. After stationary phase i.e. after 60 hours, the cfu count started to decline indicating the death phase. During death phase, nutrition requirement ceased and hence the total sugar curve became constant. Comparing the three fermentation media used it can be seen that the potato process effluent shows initial 16 g/l of total available sugar as compared to 11.3 g/l of total sugar in simulated waste

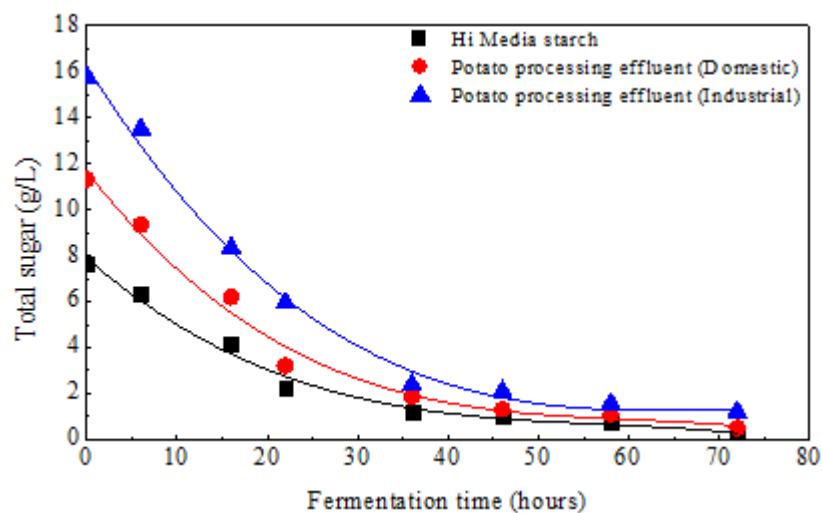


Fig. 4.5: Reduction in total sugar with time

and 7.65 g/l in purified starch media. Higher initial carbohydrate content in the potato processing effluent (industrial) must have promoted higher cell growth and higher subsequent biosurfactant – surfactin production.

It has been demonstrated by Thomson et al. (2000) that *B.subtilis* express α -amylase enzyme activity that permits the utilization of a starch-rich potato substrate as culture medium for biosurfactant production. The α -amylase activity converts the starch polysaccharide available in potato effluent substrate into simple sugars like glucose. It has been assumed in total sugar curve that the starch has been converted into glucose with the action of enzyme. This could be the reason for high microbial growth and subsequent biosurfactant production

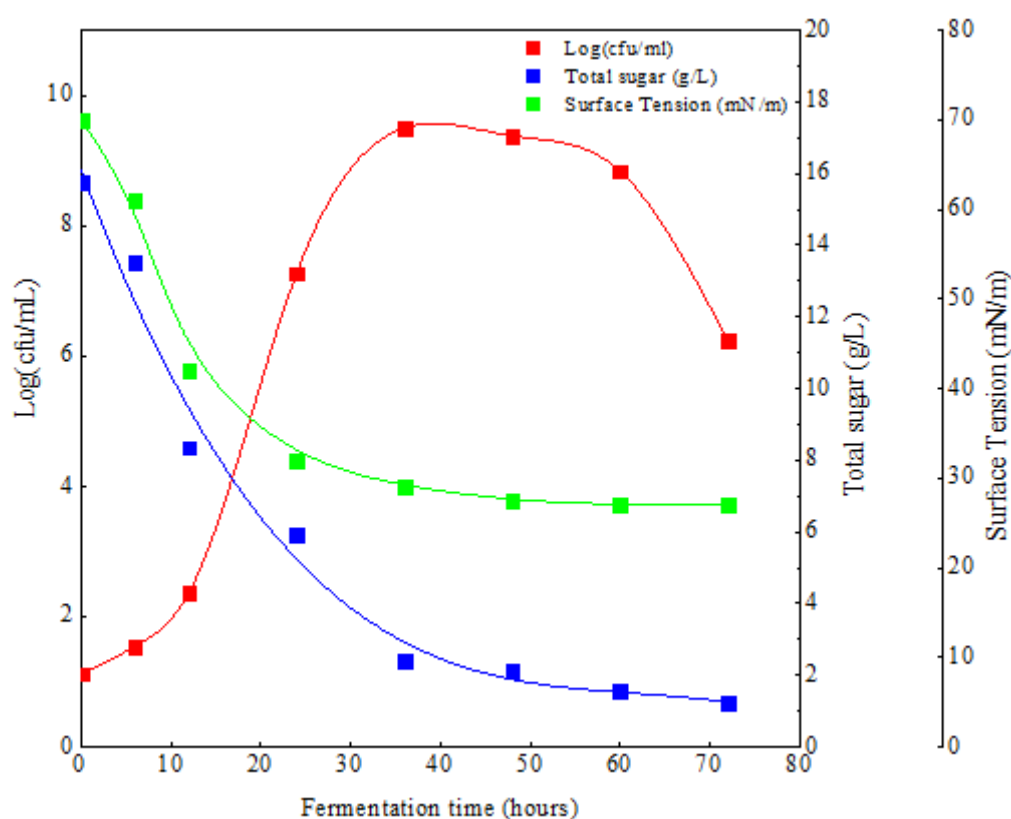


Fig. 4.6: Carbohydrate utilization, cell growth and surface tension reduction pattern observed using *B.subtilis* with potato process effluent.

From Figure 4.2 to 4.6, it was observed that the maximum surface tension reduction was observed during the exponential phase up to 36 hours, the carbohydrate utilization was also maximum up to 36 hours. The cell growth in terms of colony forming units reached maximum to $\sim 10^{10}$ cfu/ml by 36 hours of fermentation time. Therefore a relationship between carbohydrate utilization, cell growth and biosurfactant production emerges

which results in decline in the surface tension with time upto 36 hours as shown in Figure 4.6 Observation on the same lines was made by Kim et al. (1997) between surfactin production, cell growth and glucose utilization for *B.subtilis* C9. Similar observations was made earlier by Cooper et al. (1981), they reported that the production of biosurfactant-surfactin was associated with cell growth for *B.subtilis*.

4.2.5 Effect of Nutrients

Literature suggests that addition of mineral salts such as iron, magnesium, manganese and calcium to an agro substrate enhance the yield of biosurfactant. While mineral salts such as potassium, ammonium and sodium are added for obtaining rapid growth of bacterial population in the medium, addition of iron enhances the yield as well as the microbial growth (Wei and Chu, 1998). However, it has also been observed that the addition of excess quantity of iron salts leads to the acidification of the medium and as soon as the pH reduces below 5.0, the yield rapidly gets declined, suggesting that excess iron addition has a negative effect on the yield (Wei and Chu, 1998; Makkar and Cameotra, 2002; Cooper et al., 1981).

The effect of nutrients on growth of *B.subtilis* MTCC 2423 is shown in Fig. 4.4. The sample shown in red is the growth curve of substrate having identical starch concentration (2 % w/v) as sample shown in black but without inclusion of the various nutrients. It is observed that although in the first 12 hour of fermentation, bacterial growth is more when nutrients are not added to the media but thereafter the bacterial growth in black curve supersedes the growth in red curve and is nearly double at 36 h duration when peak growth is achieved in both cases.

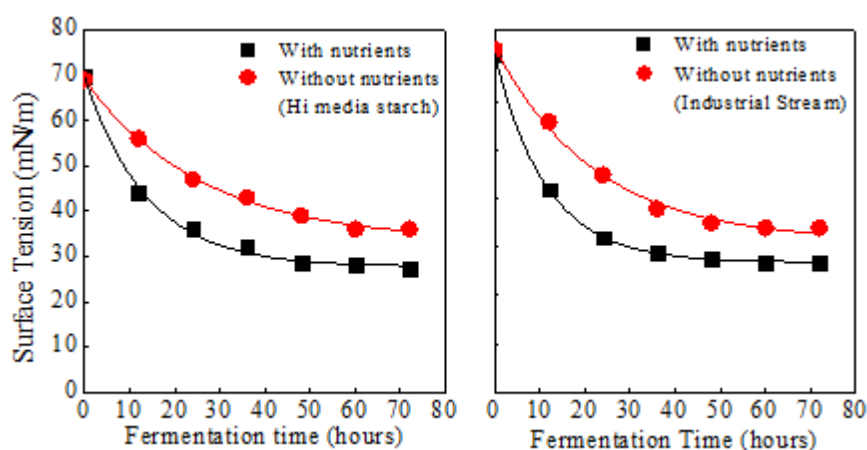


Fig. 4.7: Effect of nutrients on surface tension reduction

Biosurfactant yields are expected to be more when the bacterial growth is larger and consequently there is a greater decline of surface tension in such samples. This behavior is observed in Figure 4.7, which compares the reduction in surface tension in samples with addition of nutrients with cases where nutrients were not added.

For two cases one with dissolved Hi media starch and the other with starchy effluent water streams from Jabson Industries, it is seen that in both the cases added nutrients showed greater reduction of surface tension almost to the extent of 40%, than case where nutrients were not added. It is obvious that growth of cfu's with addition of nutrients in the media was responsible for this pattern.

4.3 Biosurfactant production using Molasses and Rice bran as substrate

4.3.1 Molasses as substrate

Molasses of different plant origin has been used as a substrate for biosurfactant production. Al-Bahry et al. (2013) used date molasses with *B. subtilis* 20 to produce biosurfactant and used it in enhanced oil recovery. Mostly rhamnolipids have been synthesized from molasses. Patel and Desai (1997) produced rhamnolipid using molasses as primary carbon source with *Pseudomonas aeruginosa* GS3 and later Raza et al. (2007) produced rhamnolipid using 2% black strap molasses and *Pseudomonas aeruginosa* EBN-8. Onbasli and Aslim (2009) used sugar beet molasses (1-5% w/v) to produce rhamnolipid surfactant wherein they used 18 strains out of which two strains *Pseudomonas luteola* B17 and *Pseudomonas putida* B12 gave the highest yields. Salehizadeh and Mohammadizad (2009) used molasses as the sole carbon source with bacterial strain *Alcaligenes sp.*MS-103 to produce extracellular lipopolysaccharide biosurfactant.

Joshi et al. (2008) studied biosurfactant production by *Bacillus licheniformis* K51, *B. subtilis* 20B, *B. subtilis* R1, and *Bacillus* strain HS3 using molasses as the sole source of nutrition at 45°C. Maximum recovery was at 5-7% w/v molasses. Al-Wahaibi et al. (2014) used date and cane molasses to produce biosurfactant using *B. subtilis* B30. In reported literature only Makkar and Cameotra (1997) used the bacterial strain *B. subtilis* MTCC 2423 with molasses as substrate for biosurfactant production and growth at 45°C, they also used the bacterial strain MTCC 1427 for fermentation of molasses to produce

biosurfactant. These investigators however did not report the chemical constituent of the biosurfactant.

In this investigation molasses was fermented using the bacterial strain *B. subtilis* MTCC 2423 the resulting biosurfactant was concentrated, isolated and appropriately characterized with the objective of testing the efficacy of molasses as substrate, identifying the biosurfactant, getting an idea of the yield in comparison with other substrates used with *B. subtilis* to obtain biosurfactants by fermentation. However, all through we were aware of the limitations of using molasses as a substrate in view of its restricted availability for commercialization in India.

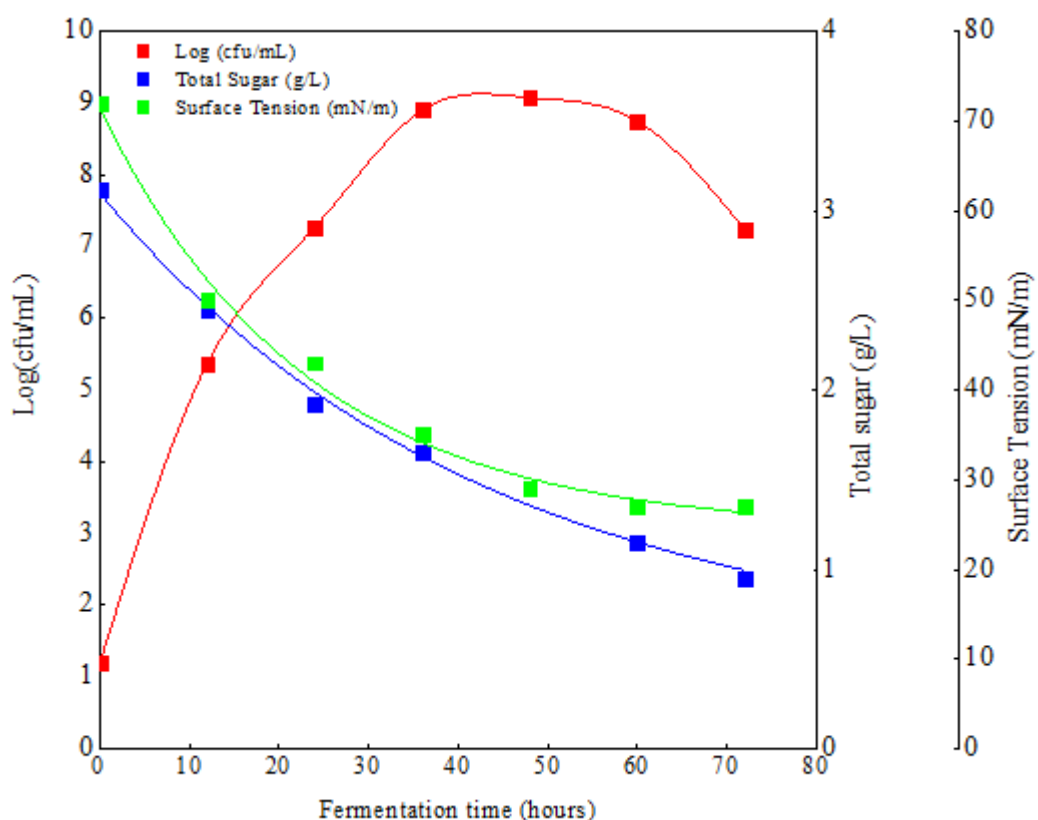


Fig 4.8: Carbohydrate utilization, cell growth and surface tension reduction pattern observed using *B.subtilis* with molasses as substrate.

The fermentation media contained 2% w/v of black strap molasses without any addition of nutrients having composition as listed in Table 4.2. The growth curve of *B.subtilis* MTCC 2423 culture in this media is shown in Figure 4.8. The colony forming units were measured with fermentation time; maximum cfu of about 10^9 was observed at 48 hour of fermentation time. The exponential phase was observed up to 40 hours of fermentation time. Thereafter, the curve went into the stationary phase which lasted up to 60 hours.

The stationary phase in case of molasses as a substrate was very small compared to that observed with potato starch.

The growth curve entered in to the death phase after 60 h of fermentation time where the cfu count reduced to around 10^7 cfu/ mL after 72 hours. It was further observed that with molasses as the substrate the total sugar reduced gradually with fermentation time. There was a decline in the sugar content even in the stationary and the death phases. The gradual decline in the sugar content even in the stationary phase could be attributed to the fact that molasses sugar consists primarily sucrose and some extent of glucose and fructose sugar. Glucose units could be released easily during fermentation by the action of α -amylase enzyme produced by the *B.subtilis* MTCC 2423 culture (Kim et al., 1997).

Molasses contains several other compounds other than sucrose such as minerals, vitamins and organic compounds that are useful for the fermentation process. Since carbon is one of the primary nutrients for cell growth, depletion of carbon source could be one of the important reasons for the decline of cell growth after 60 h of fermentation time.

4.3.2 Rice bran as substrate

The use of rice bran as a substrate for biosurfactant production is not reported in literature although it is a rich source of carbohydrates. Rice bran obtained during milling accounts for 10-12% of the weight of paddy milled. True bran amounts to only 4-5% whereas the rest is the polishing of the inner bran layers and a portion of the starchy endosperm. There is abundant amount of rice bran produced in India and almost 5 million tons is used for rice bran oil extraction and additional 4 million tons is available for processing which is currently being used as cattle feed.

In case of rice bran, the fermentation media was 2 % (w/v) slurry of uniform consistency. Experiments on the growth of the microorganism were performed as discussed in Section 3.2.3 and the colony forming units were measured as a function of fermentation time. Figure 4.9 a plot of Log (cfu/ml) versus fermentation time depicts the growth curve of *B. subtilis* in rice bran. It is evident from Fig. 4.9 that the cell growth was exponential till 24 h of fermentation time and the maximum cell growth in terms of colony forming units was $\sim 10^7$ cfu/ml. The cell growth was sustained up to 58 hours of fermentation time indicating a stationary phase from 24 hours to 58 hours. Subsequently, the cell growth

declined and entered in to the death phase. The cell growth could be associated with the availability of carbohydrate. The total sugar consumption by *B.subtilis* MTCC 2423 during fermentation with rice bran as primary carbon source is also shown in Figure. 4.9 where a continuous reduction in the available carbohydrate content with fermentation time is seen.

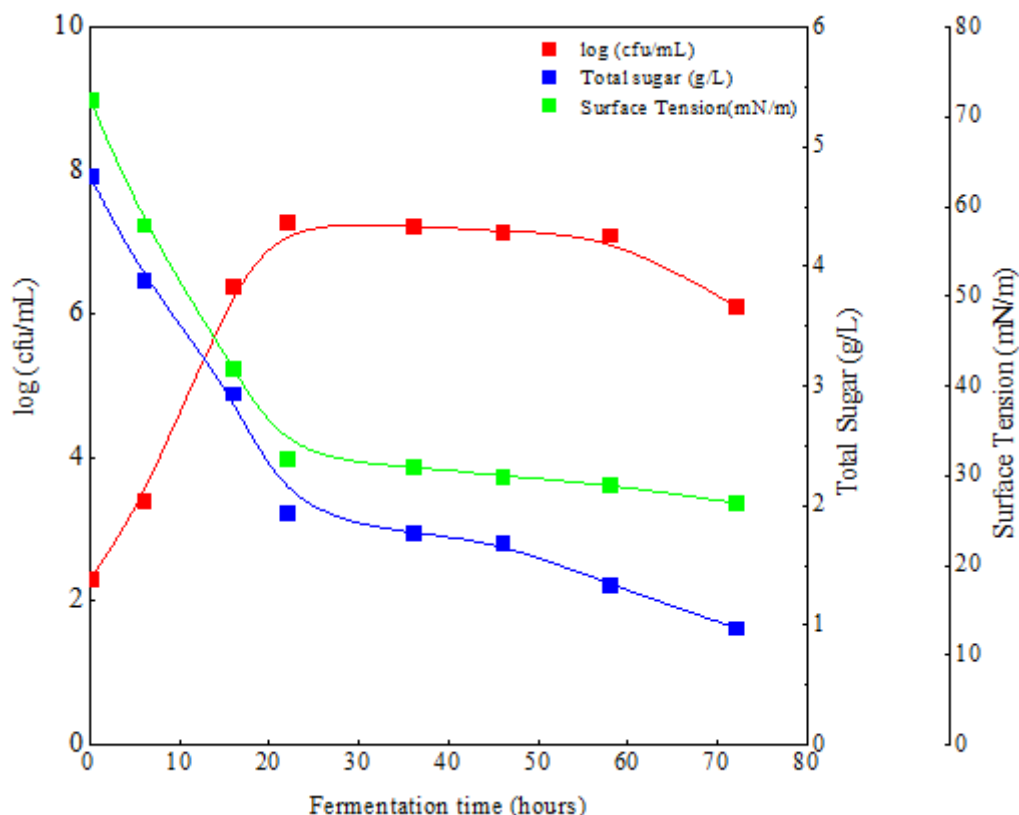


Fig. 4.9: Carbohydrate utilization, cell growth and surface tension reduction pattern observed using *B.subtilis* with rice bran as substrate.

The carbohydrate depletion was quite rapid in the initial 24 hours of fermentation time corresponding to the exponential growth phase. Thereafter during the stationary phase the rate of carbohydrate depletion slowed down considerably. The decline of cell growth after 60 hours of fermentation time could be attributed primarily to the low availability of the carbohydrate carbon source. Even after 60 hours of fermentation time, the total sugar curve was almost constant although slight reduction in sugar content was noticed because even during the death phase few organisms continue to consume sugar. The total sugar concentration measured at 72 hours of fermentation was found to be 0.98 g/l.

It is notable that the growth of *B.subtilis* in rice bran substrate took place without any external addition of nutrients; the growth was solely due to inherent nutrients present in

the media. This aspect is certainly supportive of the use of rice bran as a fermentation media for growth of *B. subtilis* and production of biosurfactant. Similar was the case with molasses, addition of nutrients was not required because of the inherent presence of such nutrients in the medium. Analysis of the fermentation media by CHN analyzer and elemental analysis by ICP yielded the results listed in Table 4.2

Table 4.2: Composition and nutrients present in rice bran and molasses

Component	Concentration in (rice bran)	Concentration in (molasses)
Total Carbohydrate (g/l)	4.76	3.12
Total Carbon % (w/w)	38.9	23
Total Nitrogen % (w/w)	28.38	36.72
Total Hydrogen % (w/w)	4.38	3.97
Iron (mg/100g)	10.12	8.419
Zinc (mg/100g)	3.79	1.242
Calcium (mg/100g)	53.14	822.8
Magnesium (mg/100g)	762.2	426.2
Manganese (mg/100g)	5.33	N.D
Potassium (mg/100g)	1323.03	3605

4.4 Surfactant concentration in the fermentation media

The concentration of biosurfactant in fermentation media can be precisely assessed when the biosurfactant is identified and liquid chromatography of the sample as well as the standard is run. Comparison of the chromatographic peaks of the standard with the surfactant sample provides the quantitative assessment of the biosurfactant concentration. However, for an initial assessment certain qualitative measures can provide working information about the concentration of the surfactant in the media.

It is well known that presence of surfactant in a solution causes the surface tension of the solution to decrease. As the surfactant concentration in solution increases the surface tension of the solution decreases until a critical concentration known as the critical micellar concentration (CMC) is reached, beyond this concentration of the surfactant in solution the surface tension does not change. If we have a surfactant solution where the concentration of the surfactant in solution is at CMC or less than CMC, then dilution of the sample would lead to an abrupt increase in surface tension since at higher dilutions, biosurfactant molecules cannot form stable micelles and the surface tension increases

abruptly. However, if the surfactant concentration is much above CMC, then even on dilution, surfactant concentration will remain above CMC and the surface tension will not change.

Hence, multifold dilution of sample gives an idea of the biosurfactant concentration in the sample relative to the CMC. Some investigators (Makkar and Cameotra, 2001) have denoted this qualitative assessment of surface tension as critical micelle dilution (CMD). It is a particularly useful index when the surfactant is likely to be used in applications where surfactant micelles play a critical role as in enhanced oil recovery.

Critical micelle dilution, a measure of the biosurfactant concentration or the dilution necessary to reach the CMC at which the surface tension starts to increase was determined for the biosurfactant produced using all the three substrates. Fig 4.10 shows the surface tension and the CMD^{-1} and CMD^{-2} reduction for the 10 times and 100 times diluted broth with time. Results show that the biosurfactant produced in the media is significant because the surface tension does not abruptly rise even on 100 times dilution. When the dilution was further increased to 1000 times there was a sharp rise in the surface tension values.

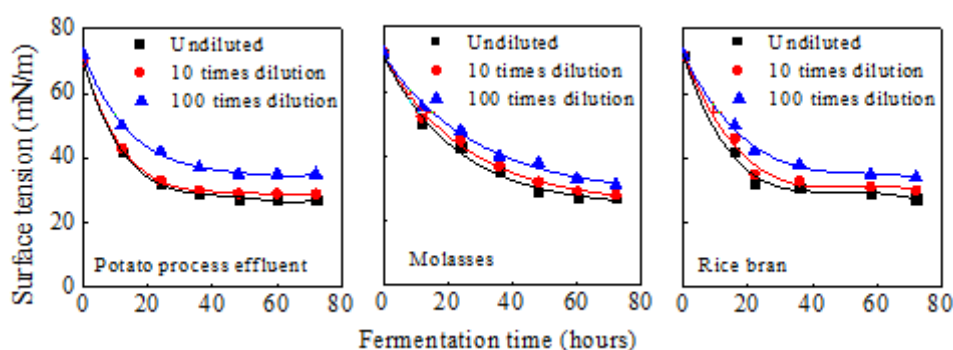


Fig. 4.10: Surface tension reduction for undiluted and diluted samples of different substrates

4.5 Growth of *B.subtilis* and modeling of growth curves

The microbial growth pattern in industrial fermentations are important not only to know the factors affecting the growth but also to develop strategies for scale up and control of the fermentation system. The growth curve is usually represented as a plot of the growth ratio N_t/N_0 (N_t represents cfu at time t and N_0 is the original cfu) or its logarithm versus time which results in a sigmoid shape curve. When conditions are held constant the pattern of growth is replicated by the microorganism at all scales of operation. Microbial

growth is extensively investigated and has been described by a variety number of mathematical models in the literature (Buchanan et al., 1997). In general the models are classified as *primary* models that describe the response of microorganisms to a single set of conditions over time, while models that describe the effect of environmental conditions on the values of the parameters of a primary model are referred to as *secondary* models. The Monod's equation which relates the microbial growth in an aqueous environment to the concentration of a limiting nutrient belongs to the class of secondary models (Carcano, 2009).

Unlike Monod's equation the Gompertz equation and the logistic equation which only describe the isothermal growth of the microorganisms and do not include the consumption of the substrate are classified as primary models. Such empirical sigmoid models that stem from statistical curve fitting exercise are usually written in terms of constants and not in terms of relevant biological parameters. Zwietering et al. (1990) in their path breaking work modified these models and interpreted the constants in terms of the biologically relevant lumped combination of parameters A , μ_m , and λ instead of mathematical entities so as to evaluate the specific growth rate, lag time and maximum growth.

Peleg and Corrandini (2011) have presented an insightful discussion on the strengths, limitations and criteria of selection of empirical phenomenological models of microbial growth and their interpretation. The oldest and the most widely used models that represent the characteristics of the sigmoid growth curve are the three parameter Logistic model and Gompertz model, shown in Equations (4.1) and (4.2) respectively. These models describe the kinetics of the microbial growth and describe with reasonable accuracy the different stages of growth. In its original form they involve the mathematical parameters a , b and c as shown in Equation (4.1) and (4.2).

Logistic equation

$$y = \frac{a}{[1+\exp(b-cx)]} \quad \dots 4.1$$

Gompertz equation

$$y = a \cdot \exp[-\exp(b - cx)] \quad \dots 4.2$$

The modified Logistic model and modified Gompertz model in terms of biologically relevant parameters are shown in Equation (4.3) and (4.4) respectively. The conversion of equation (4.1) to equation (4.3) and equation (4.2) to equation (4.4) are worked out in Appendix 2.

Modified Logistic

$$y = \frac{A}{\left[1 + \exp\left\{\frac{4\mu_m}{A}(\lambda - t) + 2\right\}\right]} \quad \dots 4.3$$

Modified Gompertz

$$y = A \exp\left[-\exp\left\{\frac{\mu_m \cdot e}{A}(\lambda - t) + 1\right\}\right] \quad \dots 4.4$$

Both the logistic model and the Gompertz model were fitted to the experimental data of growth of *B.subtilis* in the three substrates. The microbial growth data was expressed as a plot of logarithm of growth ratio $\ln(N_t / N_0)$ versus time. The non linear equations were fitted to the growth data by nonlinear regression using the Marquardt algorithm to minimize the sum of squares and difference between predicted and measured values on ORIGIN 8 platform.

Table 4.3 lists the optimized parameters a, b and c for both the Logistic and Gompertz models for growth of *B.subtilis* in all the three substrates, the goodness of fit exceeds 0.99 in all cases except for the Logistic model applied to molasses substrate. The

Table 4.3: Parameters of Logistic and Gompertz model

Substrate	Model									
	Logistic					Gompertz				
	a	b	c	R ²	RSS	a	B	c	R ²	RSS
Potato	19.815	4.437	0.223	0.999	0.0688	21.07	2.202	0.1294	0.9968	0.4865
Effluent										
Rice Bran	11.898	3.106	0.2871	0.994	0.3964	12.641	1.526	0.173	0.9996	0.0276
Molasses	17.604	2.848	0.2088	0.924	4.824	18.067	1.464	0.1358	0.992	1.496

corresponding reduced sum of squares is also shown in the Table 4.3. Figure 4.11 shows the experimental points superimposed on the sigmoid curve generated using the

parameter values obtained by curve fitting for all three substrates. The good quality of fit is also evident from Fig 4. 11.

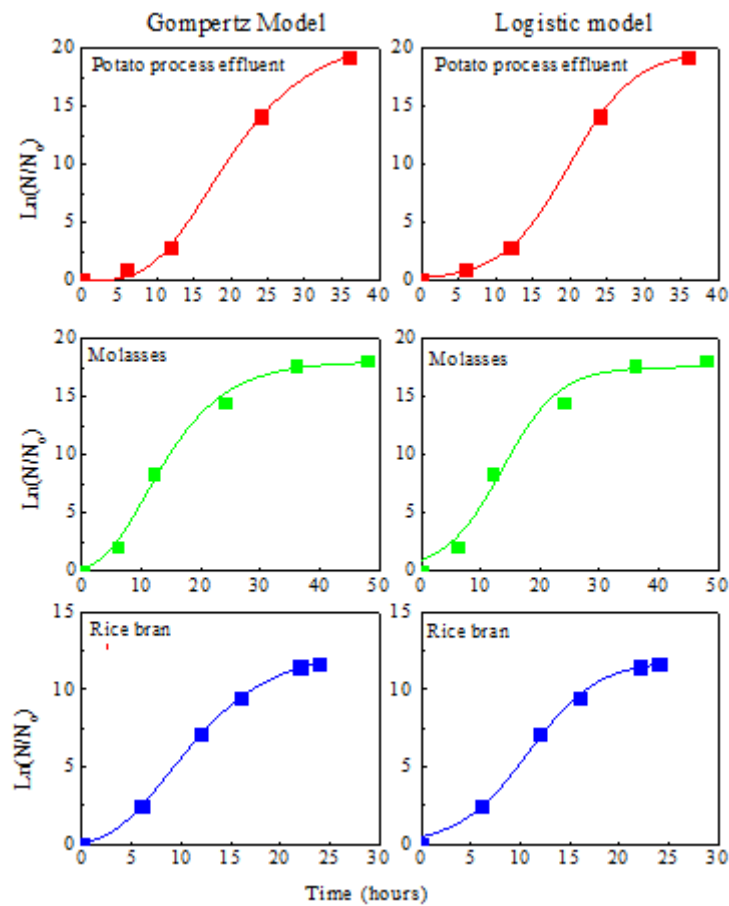


Fig. 4.11: Data fit by Logistic and Gompertz model.

The relevant biological parameters that stem out from the curve fitting parameters a , b and c are the maximum growth value reached A , maximum specific growth rate μ_{max} and lag time λ . These biological parameters describe the three phases of the growth curve and are obtained by interrelations (equation 4.5-4.7) (worked out in Appendix A2) and are listed in Table 4.4 for the three substrates.

$$A = a \quad \dots 4.5$$

$$\mu_{max} = ac/e \quad \dots 4.6$$

$$\lambda = (b-1)/c \quad \dots 4.7$$

The specific growth rate is the tangent at the inflection point, lag time is the x intercept of the tangent and the asymptote A is the maximum value reached. It is observed that the growth curve of *B. subtilis* in different substrates for different micro nutrients amounts shows almost similar specific growth rates for the three substrates but the lag times are markedly different. The lag time is the beginning of growth phase, it is a measure of the

time taken by the microorganism to adjust to the change in environment. The duration of the lag phase depends on a number of parameters such as the age, physiological state of the inoculums and on the concentration of nutrients in the media.

Table 4.4: Biological parameters from Logistic and Gompertz model

Substrate	Model					
	Logistic			Gompertz		
	Parameters					
	A	μ_{max}	λ (hrs)	A	μ_{max}	λ (hrs)
Potato Effluent	19.815	1.105	10.927	21.07	1.003	9.288
Rice Bran	11.898	0.8538	3.852	12.641	0.8049	3.041
Molasses	17.604	0.9189	4.1499	18.067	0.9026	3.42

It is observed from Table 4.4 that the lag phase of *B. subtilis* in potato starch was almost three fold longer than that observed for rice bran or molasses. This large increment is attributed to concentration of nutrients, which were naturally present in substantial amount in rice bran and molasses but had to be added externally in potato starch. It is reported in the literature that an increase in the enzyme synthesis rate shortens the lag phase (Soler, 2008), it is thus conceivable that presence of micronutrients aided the enzyme synthesis rate that led to decline of the lag period in rice bran and molasses.

4.6 Concentration of biosurfactant using foam fractionation and subsequent acid precipitation

Foam fractionation is a separation technique in which surface active solutes are concentrated from dilute solution by preferential adsorption at a gas liquid interface created by sparging an inert gas through the solution. These gas bubbles entrain the surfactant solution and form stable foam with a large gas liquid interfacial area. As foam rises through the column the surfactant solution drains due to gravity and capillary forces which results in decrease in the amount of liquid in the foam. At the top of the column the relatively dry foam is collected and broken, this results in concentration of the surface active agent. Foam fractionation has been used for concentration of proteins (Brown et al., 1999a; Brown et al., 1999b), surfactants (Hines, 1996) and has also been used to recover fermentation products from culture broths (Cooper et al., 1981). Davis et al. (2001) applied foam fractionation to downstream of cell culture stage as a separate

unit and also integrated fermentation with a system to collect the culture foam. They observed an enrichment of 51.6% and 60% respectively in both the cases.

In this work foam fractionation was used as a downstream processing technique to concentrate the biosurfactant prior to its acid precipitation to recover the biosurfactant. Foam fractionation was carried out in a fractionating column in three stages. Air was bubbled from the bottom of a column at 60 cc min^{-1} through a sinter. The foam collected from top outlet of first column was broken and the resultant foamate was fed as the input to the second column and foam collected from top outlet of second column was like wise used as the input to the third column. A sample of 100 ml fed as inlet to first column resulted in 25 ml foam collected at the top outlet of third column (Figure 4.12). Therefore, the volume reduction encountered (ratio of inlet feed to the first column to the outlet foamate from third column) was 4.0.

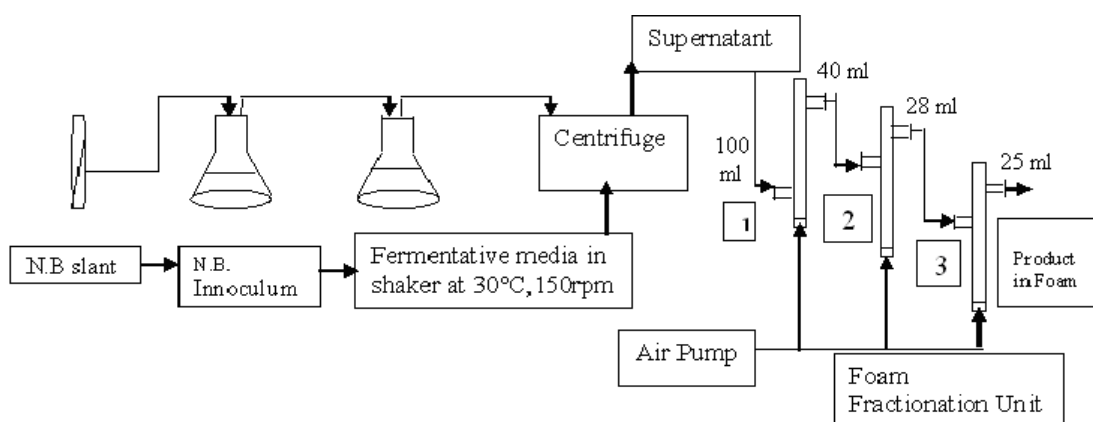


Fig. 4.12: Schematic diagram of biosurfactant production and subsequent recovery

In the first column almost 60% volume reduction was obtained i.e. from 100 ml feed sample only 40 ml was obtained as foamate while the rest 60 ml was residue. The 40 ml foamate fed to the second column resulted in a volume reduction of 30%. In the third stage the volume reduction was marginal only $\sim 11\%$. A fourth stage of foam fractionation was also tried out but all the 25 ml of feed to the fourth stage came out as foamate. Since, the fourth stage did not show any significant volume reduction it was inferred that the fourth stage was not required. Three stage foam fractionation was sufficient to concentrate the biosurfactant. The relevant recoveries of foamate in the three stages of foaming for rice bran and molasses are listed in Table 4.5.

The foam collected from top outlet of third column was subjected to acid precipitation and subsequent centrifugation. The precipitates obtained in the centrifuge tube were dried and the yield was calculated. FTIR and HPLC analysis was performed for the crude sample and concentrated foamate samples after each stage of foaming. The residual supernant solution from the three stages of foaming was mixed and subjected to acid precipitation to recover the residual biosurfactant that remained in the supernant and did not get concentrated in the foamate; these precipitates were also centrifuged and dried.

Table 4.5: Volume of foamate obtained in the three stage foam fractionation

Substrate	Initial Volume	Volume of foamate (ml)		
		1 st stage	2 nd stage	3 rd stage
Rice bran	1000ml	405	282	250
Molasses		330	221	200

The yield of biosurfactant using *B.subtilis* MTCC 2423 from the three substrates of agriculture origin is listed in the Table 4.6. The yield from rice bran and molasses are expressed as per unit mass of the substrate, while from potato washings and other sources of potato starch its expressed as per unit volume. It is observed that the net yield of the biosurfactant was in the order rice bran > molasses > potato.

Table 4.6: Yield of biosurfactant produced on precipitation from foamate.

Substrate	Potato starch			Rice bran			Molasses		
	Hi Media	House hold waste	Industrial effluent	Foamate Conc. mg/L	Residue mg/L	Net Yield Per unit mass of substrate	Fomate Conc. mg/L	Residue mg/L	Net Yield Per unit mass of substrate
Yield	0.78g/L	1.15g/L	1.76 g/L	238.8	35.46	4.3g/kg	190.4	22.4	2.8g/kg

Table 4.6 also shows the concentration of the biosurfactant in the foamate as well as the residual solution. The foamate volume is 25% of the initial feed volume for rice bran and 20% of the volume for molasses, it is found that 69.2% of the biosurfactant is recovered in foamate from rice bran and 68% is recovered in the foamate in case of molasses. Hence the recoverable yields turn out to be 2.985 g/kg for rice bran and 1.904g/kg for molasses. Comparing the values listed in Table 4.1 it is found that the yield of the

biosurfactant obtained in this investigation with the industrial potato starch effluent, molasses and rice bran is very much in the range. In fact the recoverable yield from rice bran is superior to the yields reported in the literature for various agricultural substrates while that from molasses is equivalent to reported yields.

It should be noted that we have compared based on recoverable yields from foamate only. In fact the net yields i.e. from foamate and residual are very much superior to any such values reported in the literature with *B. subtilis*. We have restrained from comparing the net yield obtained in view of the fact that for acid precipitation very strong acid is required to make the precipitation environment highly acidic, particularly so to precipitate the biosurfactant from the residual solution where the volume of solution is large and surfactant concentration is quite low. Such acid precipitation of residual solution is possible in the laboratory scale but in an operational scale the environmental load makes this recovery by precipitation impractical and unfeasible. However, since almost 30% of the total biosurfactant synthesized remains in the residual solution it seems appropriate to further concentrate the biosurfactant using appropriate membrane separation technique to enhance the recovery and the yield of the biosurfactant product.

The total yield of the biosurfactant from rice bran and molasses varied widely in spite of the fact that during fermentation both rice bran and molasses were prepared utilizing 2 % (w/v) as substrate in the initial media. It was quite evident from Table 4.2 that the availability of nutrients in the rice bran and molasses as well as the carbon source played a vital role in defining yield of the biosurfactant. The total carbon percentage (w/w) basis in rice bran was 15.9 % higher as compared to carbon percentage in molasses. The total carbohydrate content calculated was also higher in rice bran fermentation media as compared with that of the molasses fermentation media. The contribution of mineral salts towards the yield of biosurfactant has been reported earlier by different authors. The concentration of important mineral salts such as iron, magnesium, calcium and manganese were determined in rice bran and molasses in this investigation and is reported in Table 4.3.

Makkar and Cameotra. (2002) found that the Mg^{2+} had an influence on the yield of biosurfactant and concentration of 2.43 mM Mg^{2+} in the media increased the yield of biosurfactant. $CaCl_2$ at 0.36 mM concentration resulted in optimal biosurfactant yield. As

reported by Cooper et al. (1981), addition of $MnSO_4$ salt played significant role in increasing the yield of surfactin.

Wei and Chu. (1998) have reported that the production of the surfactin by *B.subtilis* MTCC 2423 was dramatically enhanced by the addition of iron sulfate at different stages of cell growth. The yield of surfactin in this way could be raised to several hundred mg/ L by iron addition to the fermentation medium. Iron enrichment also supported microbial growth and raised biomass concentration. The results of present work indicate that the yield of biosurfactant with rice bran as substrate was higher than the yield obtained with molasses and this could also be attributed to the higher iron content in rice bran as compared to that in the molasses as seen in Table 4.2. The concentration of magnesium was also higher in rice bran compared to its concentration in molasses.

Magnesium being an important ingredient for biosurfactant yield, rice bran as substrate was ideal since it contained sufficient quantity of magnesium. Rice bran therefore had all the key nutrients that were necessary for the good yield of biosurfactant in sufficient quantity when compared with the nutrients available in molasses. The yield of biosurfactant observed in fermentation with rice bran was therefore higher compared to molasses as substrate.

4.7 Characterization of synthesized biosurfactant:

Biosurfactants are structurally complex molecules having high molecular weights. They are synthesized by variety of microorganisms and are usually not obtained singularly but in mixtures of isoforms having nearly identical structures and molecular weights. Hence, their purification, identification and characterisation are tedious and involve highly elaborate procedures and analytical techniques. The best characterized lipopeptide till date is surfactin shown in Figure 4.13, it is a mixture of cyclic lipopeptide isoforms

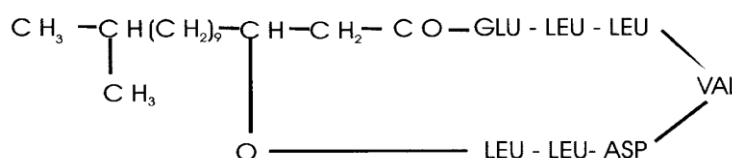


Fig. 4.13: Structure of Surfactin (Kakinuma et al., 1969)

(homologs) differing in the length and branching of the fatty acid side chains and in the amino acid substitutions in the peptide ring. The active component is a mixture of C₁₂-C₁₅ isomers. Different strains of *Bacillus subtilis* produce different lipopeptide family and also lipopeptides with different peptide cores like surfactin and iturin. (Bonmatin et al.,2003). *Bacillus subtilis* usually produces surfactin like lipopeptides and there are a number of techniques of varying degree of sophistication used for their characterization. These techniques include TLC, FTIR, NMR for chemical group identification, HPLC for identification and purification, ESIMS, GCMS, FAB-MS are used to determine fatty acid content, the peptide sequence and for molecular weight determination.

In addition to the above mentioned techniques, physical techniques such as surface tension gives information of ST reduction and micellization behaviour, dynamic light scattering (DLS) techniques estimate the hydrodynamic radius (*R*) of the surfactant micelles giving the size of micelle. Microscopic techniques such as transmission electron microscopy (TEM), Cryo-TEM, are used for the characterization of shape and the size of micelles. Small-angle neutron scattering (SANS) and small-angle X-ray scattering (SXAS) are useful for the determination of molecular weight, radius of gyration, core radius of micelle and macrolattice structures. Combining the information obtained from all these techniques help infer the complete structure of the molecule.

In the current investigation, chemical characterization of the biosurfactant was done by TLC, FTIR, and NMR. ESIMS/MS was used to determine the molecular weight and the peptide sequence. Surface tension was used throughout the study for general purpose and finally DLS was used to estimate of the size of surfactin micelles formed in solution.

4.7.1 Thin Layer Chromatography (TLC)

Thin Layer Chromatography (TLC) is a relatively inexpensive technique to detect biosurfactants, it is based on the principle of solutes competing with solvent for surface sites on adsorbent. Spot detection of samples from TLC plate can be done using destructive or non-destructive tests. Different developers are used to detect carbohydrates, lipids and proteins. A detailed summary of the different solvent systems and developers used for characterization of biosurfactant by TLC is reviewed by Satpute et al. (2010) In this study foam collected from third stage of foam fractionation after disintegration was subjected to Thin Layer Chromatography. The components of the

liquid were separated on silica gel - 60 plates using solvent system of n-butanol-acetic acid-water in the optimized proportion of 12: 3: 5 respectively. Silica gel plates (a), (b) and (c) was prepared for TLC under identical conditions when rice bran was used as the substrate. The plates after chromatography were allowed to dry for further detection of the components. Presence of a spot/ band on the plate after development using appropriate developers/techniques is indicative of a positive result.

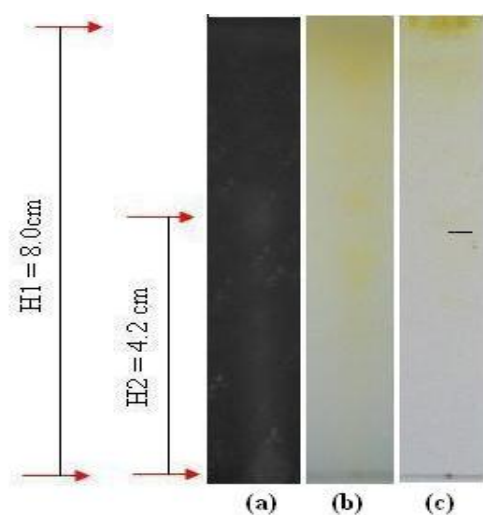


Fig. 4.14: TLC identification of Lipopeptide: Spot visible on the plates at height 4.2 cm. (a) Plate observed under UV lamp at 254 nm, (b) Plate observed after development with iodine vapours for rice bran, (c) Plate observed after development with iodine vapors for molasses.

On the TLC plate (a) in a UV chamber under UV lamp at 254 nm a band was revealed at height H_2 (Figure 4.14), which is indicative of the presence of a lipopeptide (Mukherjee et al., 2008). The same biosurfactant sample, stained yellow spot on TLC plate (b) on development with iodine vapour again at height H_2 as in plate (a) revealing the presence of lipid in the molecule (Mukherjee et al., 2008) (Figure 4.14). TLC plate (c) also stained yellow in presence of iodine vapors and showed spots at almost similar height when molasses was used as the substrate. Since these spots were observed at similar heights on both the plates one can infer the presence of both lipid and peptide moiety in the same molecule confirming its lipopeptide nature.

The retention factor R_f was found as a ratio of H_2/H_1 which turned out to be 0.525 and 0.52 when using rice bran and molasses as substrate respectively. Similar values for retention factor were observed by Kowall et al. (1998) and Mukherjee et al. (2008) for lipopeptide biosurfactant, surfactin.

4.7.2 FTIR analysis

Preliminary characterisation was done by FTIR to identify the representative functional groups present and the chemical nature of the biosurfactant. The IR spectra of the crude biosurfactant obtained from molasses and its subsequent concentrated and purified form using foam fractionation is shown in Figure 4.15. It is seen that as the number of fractionation stages increases, the bands representing the constituent of the surfactant became more prominent and sharper, which is attributed to an increase in the concentration of the active component,

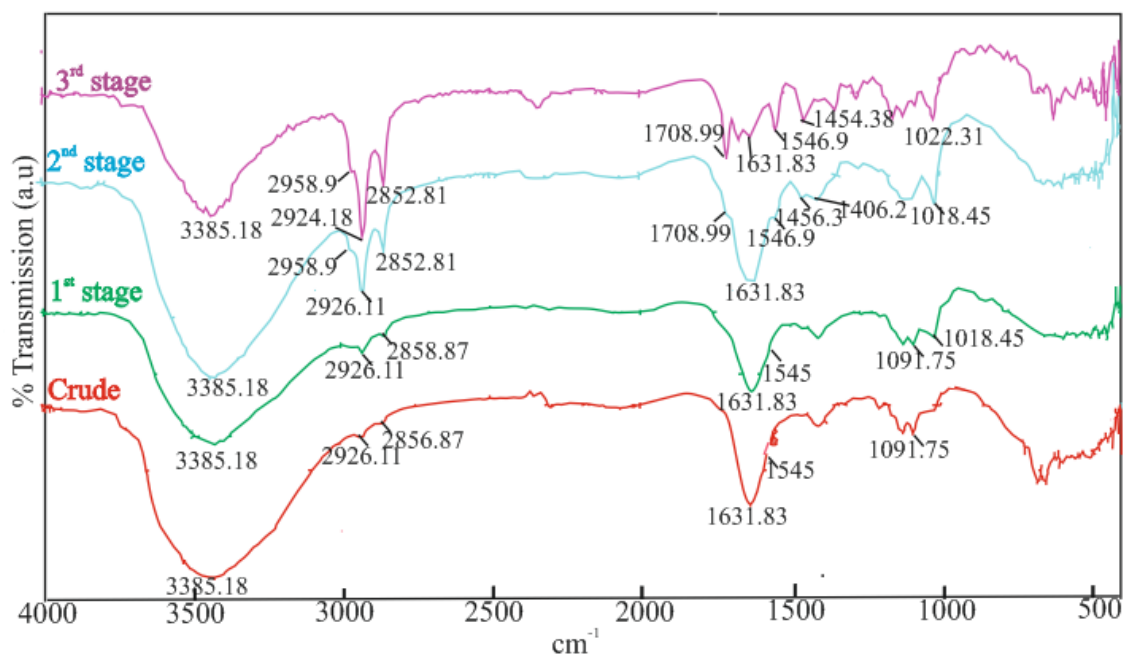


Fig. 4.15: IR spectra of crude and concentrated biosurfactant obtained from molasses

The spectra showed strong absorption bands at 3315.18 cm^{-1} , indicating the presence of peptide component due to the N–H and O–H stretching vibrations. The bands at 2958.9 cm^{-1} , 2924.18 cm^{-1} , 2852.81 cm^{-1} indicate the presence of an aliphatic chain in the biosurfactant. The band centred at 1454.38 cm^{-1} corresponds to the CH_2 bending of lipids. The peak at 1708.99 cm^{-1} showed the presence of an ester carbonyl. The band at 1546.9 cm^{-1} assigned to the amide II bonds arises from N–H bending and C–N stretching. These results indicate that the biosurfactant contains both aliphatic and peptides like moieties. Similar results have been reported by some investigators (Makkar and Cameotra, 1999) for surfactin and all the peaks that benchmark surfactin are identified in the IR spectra of the third foamate.

Figure 4.16 shows the IR spectra of the crude and concentrated biosurfactant synthesized using rice bran as the substrate. The spectra showed strong absorption bands at

$\sim 3329.25\text{cm}^{-1}$, indicating the presence of a peptide component due to the N–H and O–H stretching vibrations. The bands at 2966.6 cm^{-1} , 2928.04 cm^{-1} , 2858.6 cm^{-1} indicate the presence of an aliphatic chain in the synthesized biosurfactant. The band centered 1404.22cm^{-1} corresponds to the CH_2 bending of lipids. However, the intensity of the ester carbonyl band at 1709 cm^{-1} and the amide II bands arising from N–H bending and C–N stretching at $\sim 1587\text{ cm}^{-1}$ were very low. The presence of all these bands also indicates that the biosurfactant contained both aliphatic and peptides like moieties. In comparison with the IR spectra of the third foamate sample using molasses, the intensities of the IR peaks of the third foamate of rice bran were relatively lower which could be attributed to the concentration of the active component in the initial samples.

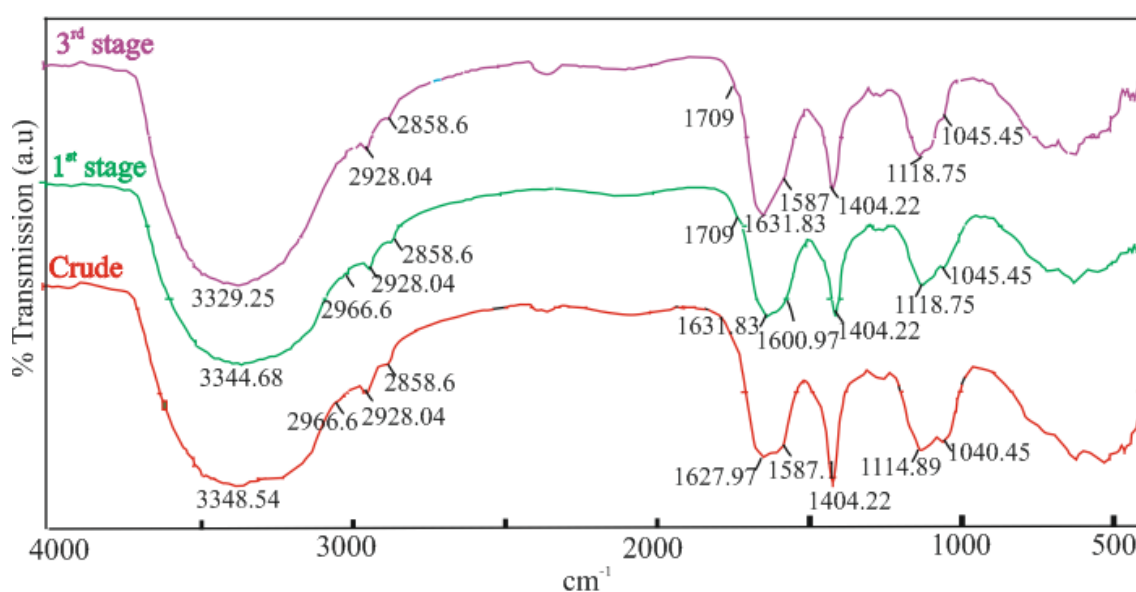


Fig.4.16: IR spectra of crude and concentrated biosurfactant obtained from rice bran

4.7.3 Nuclear magnetic resonance spectroscopy (NMR)

The characterization of biosurfactant produced by *Bacillus subtilis* strains using NMR spectroscopy has been discussed by Peypoux et al. (1991), Kowall et al. (1998), Liu et al. (2009). NMR provides information regarding the functional groups as well as the position of the linkages within the carbohydrate and lipid molecules. Identical functional groups with differing neighbouring substituent give unique distinguishing signals. Exact location of each functional group can be obtained and information about the structural isomers can also be gathered with the help of a series of NMR experiments.

The biosurfactant after foam fractionation and subsequent acid precipitation was further hydrolyzed by using 6N HCL. The hydrolysis facilitates the opening of the peptide bond

between the amino acid units releasing free amino acid residues and fatty acid residues from the cyclic lipopeptide structure. The hydrolyzed sample was dissolved in dimethylsulfoxide and subjected to ^1H NMR spectroscopy. The chemical shifts were referenced to the residual dimethylsulfoxide resonance at 2.49 ppm.

The ^1H NMR spectra for the hydrolyzed biosurfactant samples, obtained from molasses as well as rice bran as the substrate are shown in Figure 4.17a and 4.17b respectively. The standard ^1H NMR spectrum for surfactin shows three main regions corresponding to the resonances of amide protons (6.5-10 ppm), α -carbon protons (3.5-5.5 ppm) and the side chain protons (0.25-3.0 ppm) Pereira et al.(2013).

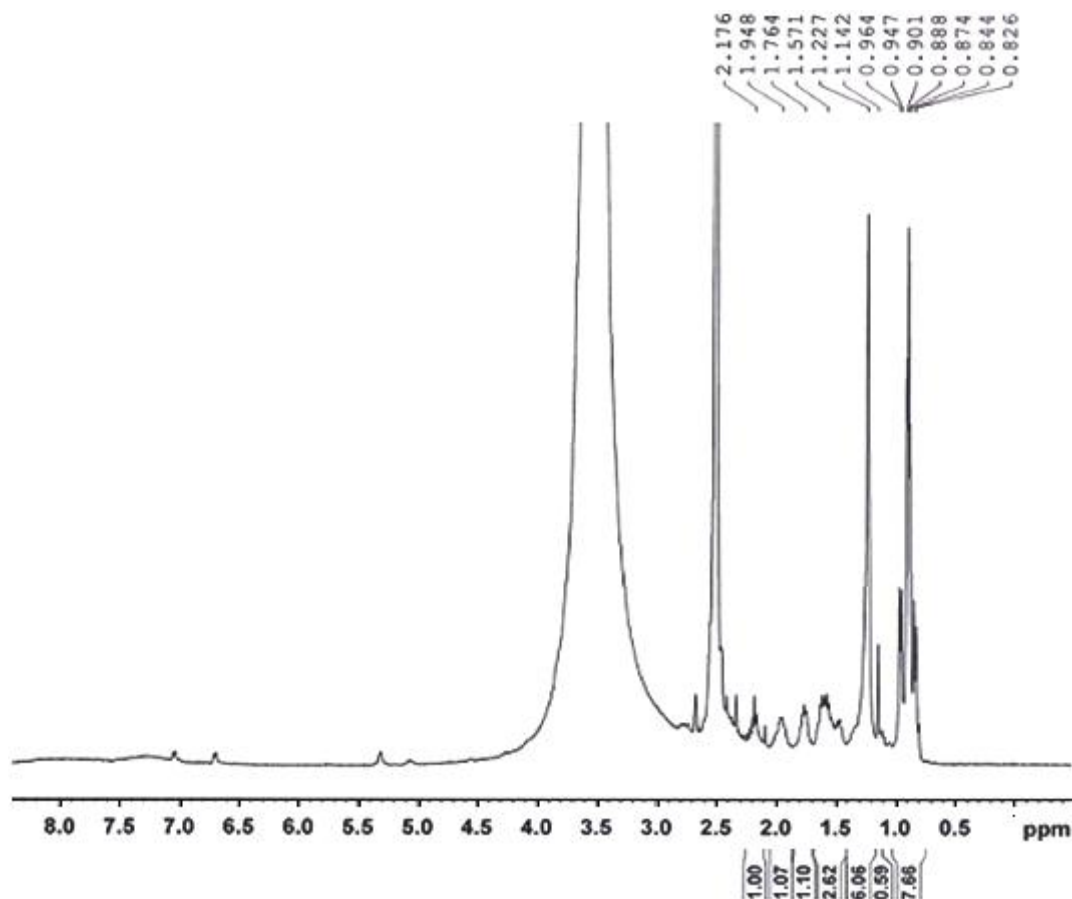


Fig.4.17a: ^1H NMR spectra for surfactin produced by *B. subtilis* from molasses (after acid hydrolysis)

A large signal at 1.22 ppm indicates the presence of the fatty acid side chain. This result was in consonance with the results reported by Peypoux et al. (1994), Tang et al. (2007). The resonance at 5.3 ppm corresponds to the terminal proton of the fatty acid chain. This resonance was also observed by (Liu et al., 2009; Pereira et al., 2012) during separation and characterization of surfactin isoforms. Few low intensity peaks were observed in the amide region between 7 and 7.5 ppm, corresponding to leucine amino acid at 3rd and 6th

position in heptapeptide sequence. However, amide shifts corresponding to all amino acids were not visible as these can be seen in the NMR spectra only when the hydrolysis is complete leading to breakage of the peptide bonds. The α -carbon proton shifts in the region between 4.0-4.5 ppm were not observed for the same reason. Fig.4.18 shows the NMR of the non hydrolysed surfactin sample which shows the non existence of the α -carbon and there are no shifts visible in the amide region, suggesting that hydrolysis did not occur at each peptide bond of the heptapeptide amino acid sequence in surfactin molecule.

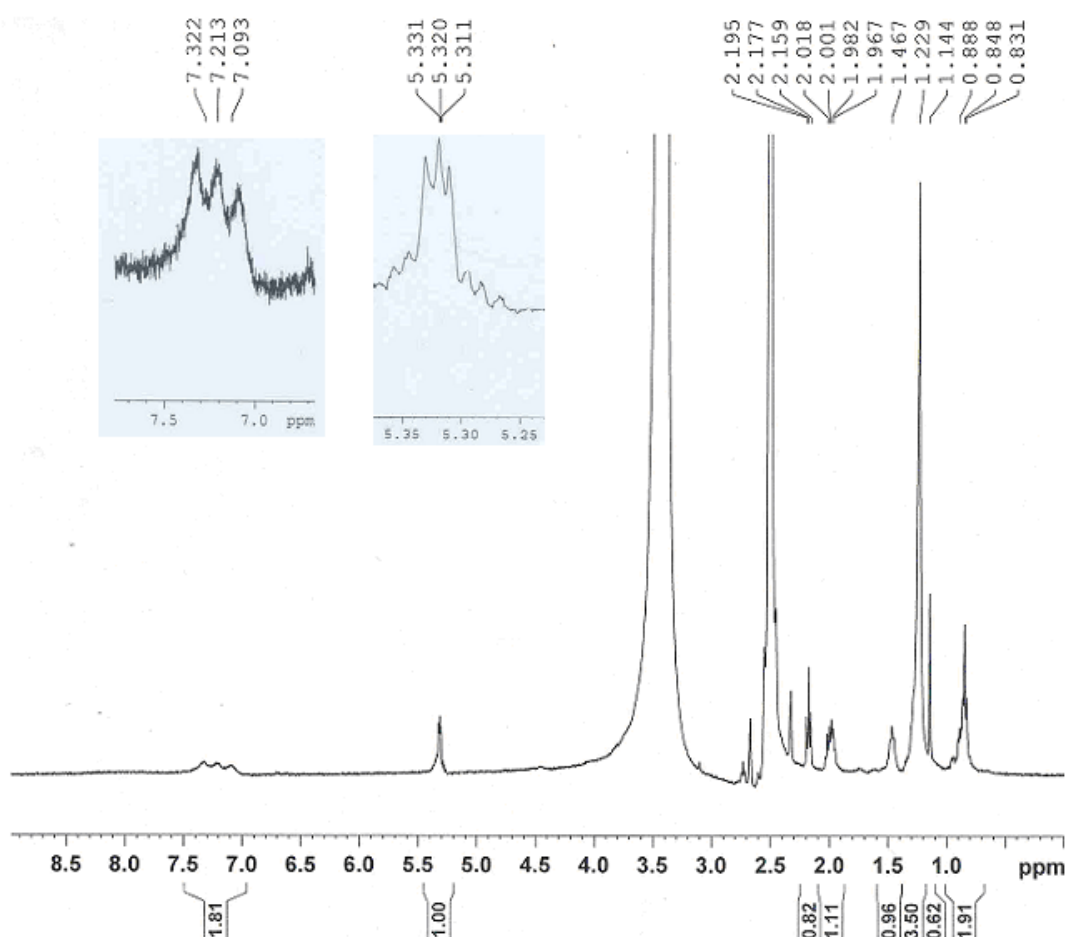


Fig.4.17b: ¹H NMR spectra for surfactin produced by *B. subtilis* from rice bran (after acid hydrolysis)

Few low intensity peaks were observed in the amide region between 7 and 7.5 ppm, corresponding to leucine amino acid at 3rd and 6th position in heptapeptide sequence. However, amide shifts corresponding to all amino acids were not visible as these can be seen in the NMR spectra only when the hydrolysis is complete leading to breakage of the peptide bonds. The α -carbon proton shifts in the region between 4.0-4.5 ppm were not observed for the same reason. Fig.4.18 shows the NMR of the non hydrolysed surfactin

sample which shows the non-existence of the α -carbon and there are no shifts visible in the amide region, suggesting that hydrolysis did not occur at each peptide bond of the heptapeptide amino acid sequence in surfactin molecule.

The β -H signals in the NMR spectra obtained at 1.967, 1.467, 1.47, 2.177, 2.57, 1.47, 2.00 corresponds to residue –Glutamic acid(1), Leucine(2), Leucine(3), Valine(4), Aspartate(5), Leucine(6),Isoleucine(7). The γ -H signals of six amino acid residues were observed at 1.96, 1.46, 1.46, 0.88, 1.14 and 0.83 ppm. The δ -H signal at 0.84, 0.84, 0.83 and 0.83 were observed for leucine(2), leucine(3), leucine(6) and Isoleucine/leucine(7) respectively. All these shifts were also observed in the non hydrolysed sample.

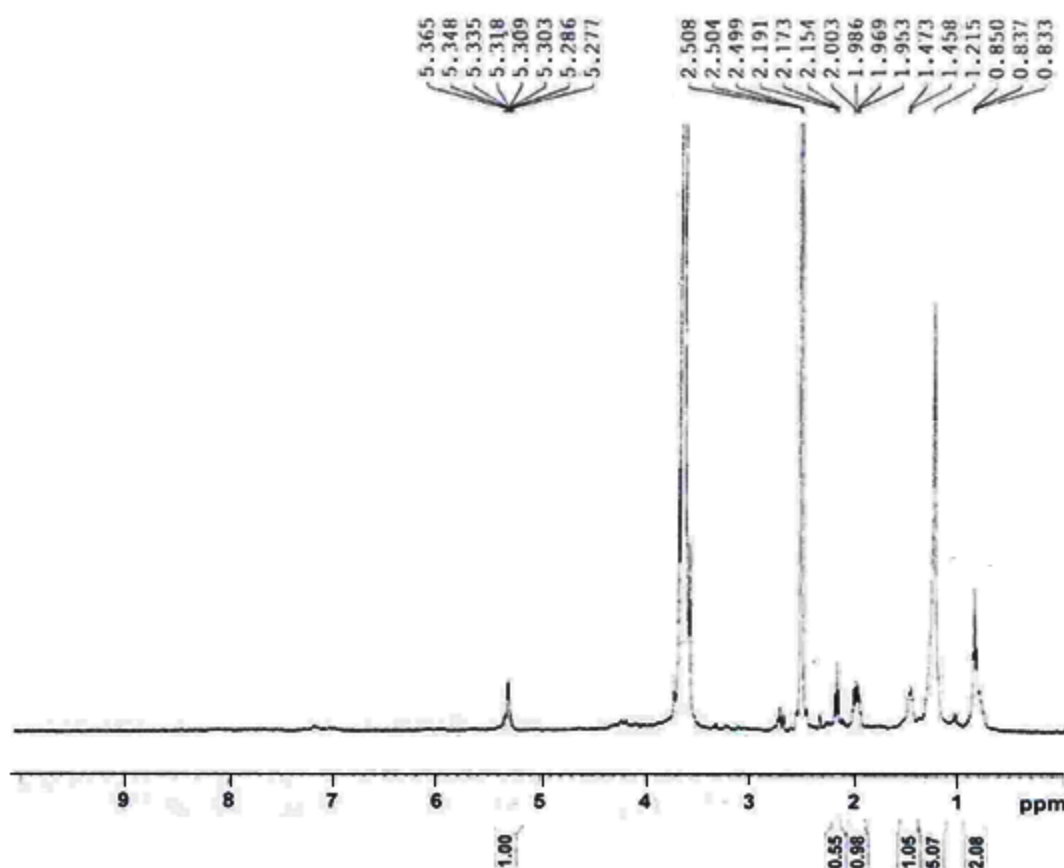


Fig.4.18: ^1H NMR spectra for surfactin produced by *B. subtilis* from rice bran (without acid hydrolysis)

The NMR spectra for molasses also exhibited similar spectra with hydrolysis occurring only at specific locations in the heptapeptide sequence. The β -H signals were obtained at 1.948, 1.57, 1.57, 2.176, 1.57, 2.17 corresponding to residue – Glutamic acid(1), Leucine(2), Leucine(3), Valine(4), Leucine(6), Isoleucine(7). The γ -H signals of six amino acid residues were observed at 1.948, 1.57, 1.57, 0.88, 1.142 and 0.826 ppm. The

δ -H signal at 0.84, 0.84, 0.826 and 0.826 were observed for leucine(2), leucine(3), leucine(6) and Isoleucine/leucine(7) respectively.

4.7.4 High Performance Liquid Chromatography (HPLC)

The separation and / or purification of lipopeptide type surfactants could be achieved by the HPLC technique. (Liu et al., 2009; Wei and Chu, 1998). Separation of various components of the feed is based on their polarity, the separated products can be detected and fractions representing individual peaks can be collected to analyze the structure of each moiety. Since surfactin exists in various isoforms its quantification is quite complex. HPLC coupled with tandem mass spectrometry (HPLC-MS) has also been used by investigators to detect surfactin isoforms (Tang et al., 2010).

HPLC of the product obtained by the fermentation of rice bran and molasses was conducted using 3.8 mM trifluoroacetic acid (20%) and acetonitrile (80%) as the mobile phase with the objective of judging the effectiveness of foam separation as a concentration and purification technique as well as identifying the product. It is seen from Fig.4.19a and 4.19b that the intensity of the peaks at specific retention times progressively increases with an increase in number of stages of foam fractionation, some minor peaks totally disappear in the final concentrate, indicating that there is an increase in the purity as well as concentration of the product during the multistage foam fractionation recovery process. However the identity of the individual peaks was not investigated further

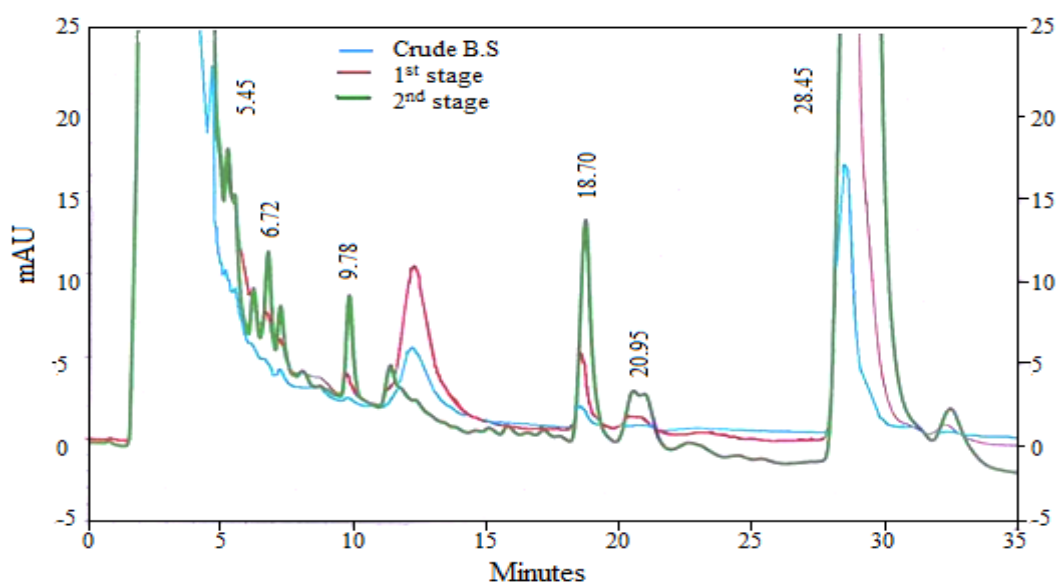


Fig.4.19a: HPLC plots indicating purification and concentration of surfactin (Rice bran)

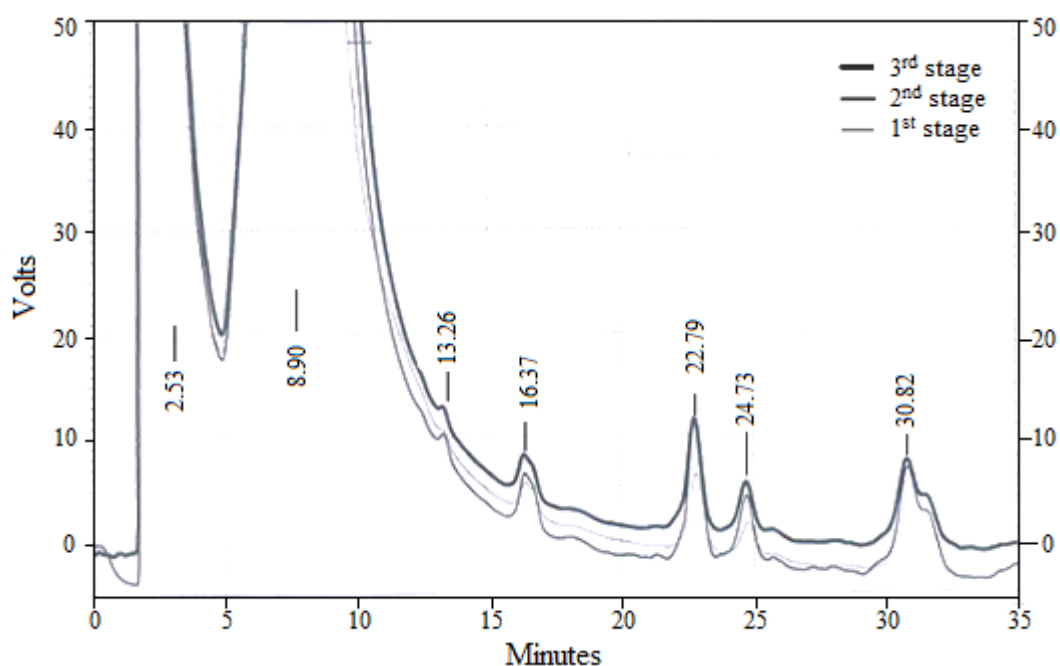


Fig. 4.19b: HPLC plots indicting purification and concentration of surfactin (Molasses)

Wei and Chu (1998) have reported the HPLC spectra of surfactin (Sigma) using the same mobile phase consisting of 3.8 mM trifluoroacetic acid (20%) and acetonitrile (80%) and identified a total 30 peaks in the spectra. Table 4.7 lists the major peaks identified in the HPLC spectra of the product obtained by fermentation of rice bran and molasses in this study in comparison with the peaks listed by Wei and Chu. There is remarkable closeness of match between the major peaks reported by Wei and Chu (1998) and those observed in our HPLC spectra for product obtained from rice bran although relative intensities are different, which is attributed to presence of different isoforms in the sample. This leaves little doubt that the product obtained by fermentation of rice bran by BS is surfactin. Similar is the case for product obtained from molasses however, the isoforms of surfactin obtained from rice bran and molasses appear to be different.

Table 4.7a: Retention peaks in HPLC spectrogram of surfactin obtained from rice bran compared with commercial surfactin (Sigma) reported by Wei and Chu (1998).

Surfactin (Sigma)	0.64	2.54	3.60	5.33	5.92	6.96	8.46	11.18
Surfactin (Rice bran)	0.73	2.46	3.72	5.43	6.17	6.72	8.72	11.37
Surfactin (Sigma)	12.22	15.04	15.45	16.56	17.20	17.98	20.88	28.58
Surfactin (Rice bran)	12.31	15.13	15.83	16.59	17.19	17.76	20.98	28.56

Table 4.7b: Retention peaks in HPLC spectrogram of surfactin obtained from molasses compared with commercial surfactin (Sigma) reported by Wei and Chu (1998).

Surfactin (Sigma)	1.161	2.54	8.46	13.96	16.56	17.98	20.57	23.09	25.88	28.58
Surfactin (Molasses)	1.02	2.53	8.90	13.26	16.34	17.92	21.38	22.79	25.65	28.06

4.7.5 Electrospray Ionization Mass Spectrometry (ESI-MS)

High molecular weight biosurfactants like surfactin are structurally complex. These lipopeptides are analysed by mass spectrometry, colorimetric and sequencing analysis. Fatty acid content and the peptide sequence are determined by mass spectrometry. Combination techniques are required for complete structure analysis.

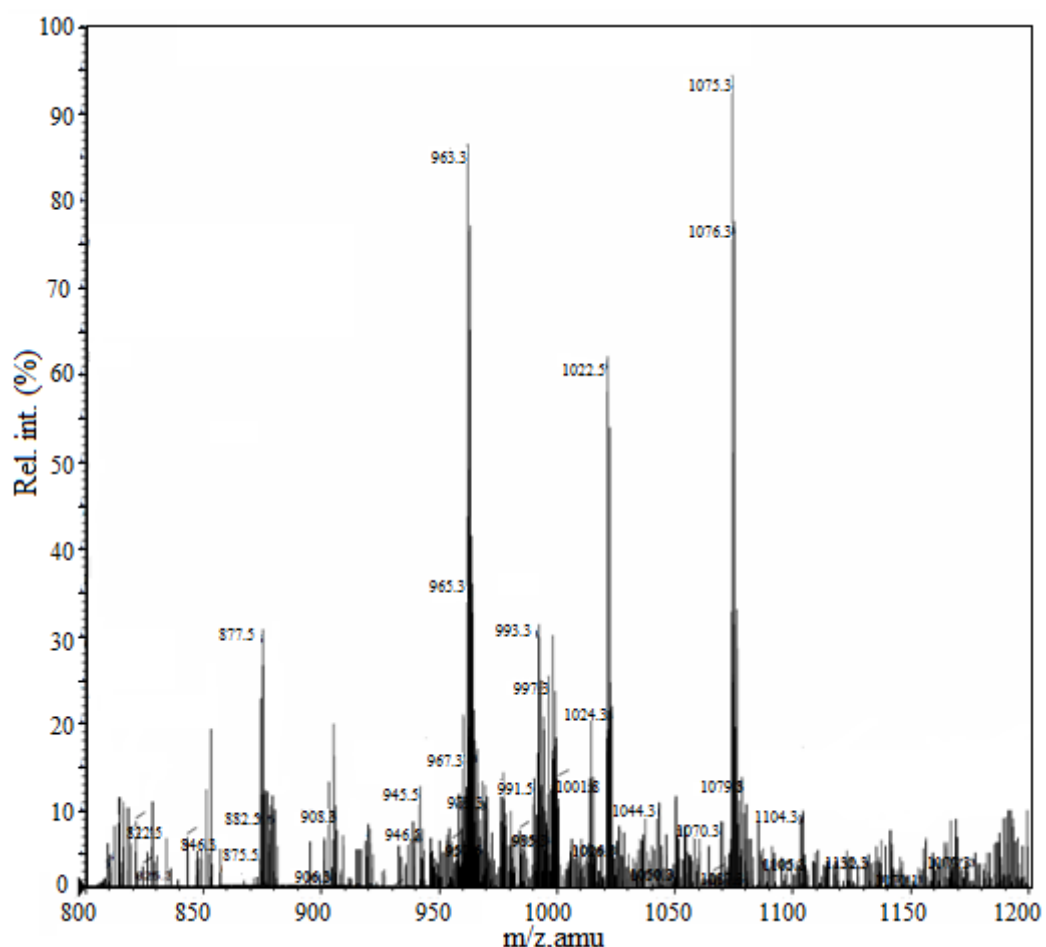


Fig 4.20: ESI-MS of the surfactin obtained from rice bran showing $[M+H]^+$ peaks

Sample for ESI-MS was prepared as discussed in Chapter 3 and was subjected to positive ion ESI-MS. The prominent $[M+H]^+$ peaks were observed at m/z 963.3, 994.3, 1022.5, 1036, 1044.3, 1050, and 1075.3 for surfactin obtained from rice bran (Figure

4.20). The fragmentation behaviour of two isoforms 1075.8 and 1022.5 was further investigated by performing MS² spectra. The MS² (Figure 4.21) showed that the fragmentation route of 1075.8 and 1022.5 were similar and was dominated by a common ion peak at m/z 685.7. The peak m/z at 685.7 strongly corresponds to peptide component of surfactin (Makkar and Cameotra, 1999). The presence of this ion also indicates the preferential opening of the ring at the ester site (Figure 4.22 a), this is in consistence with results reported by Tang et al. (2010) and Romano et al. (2011).

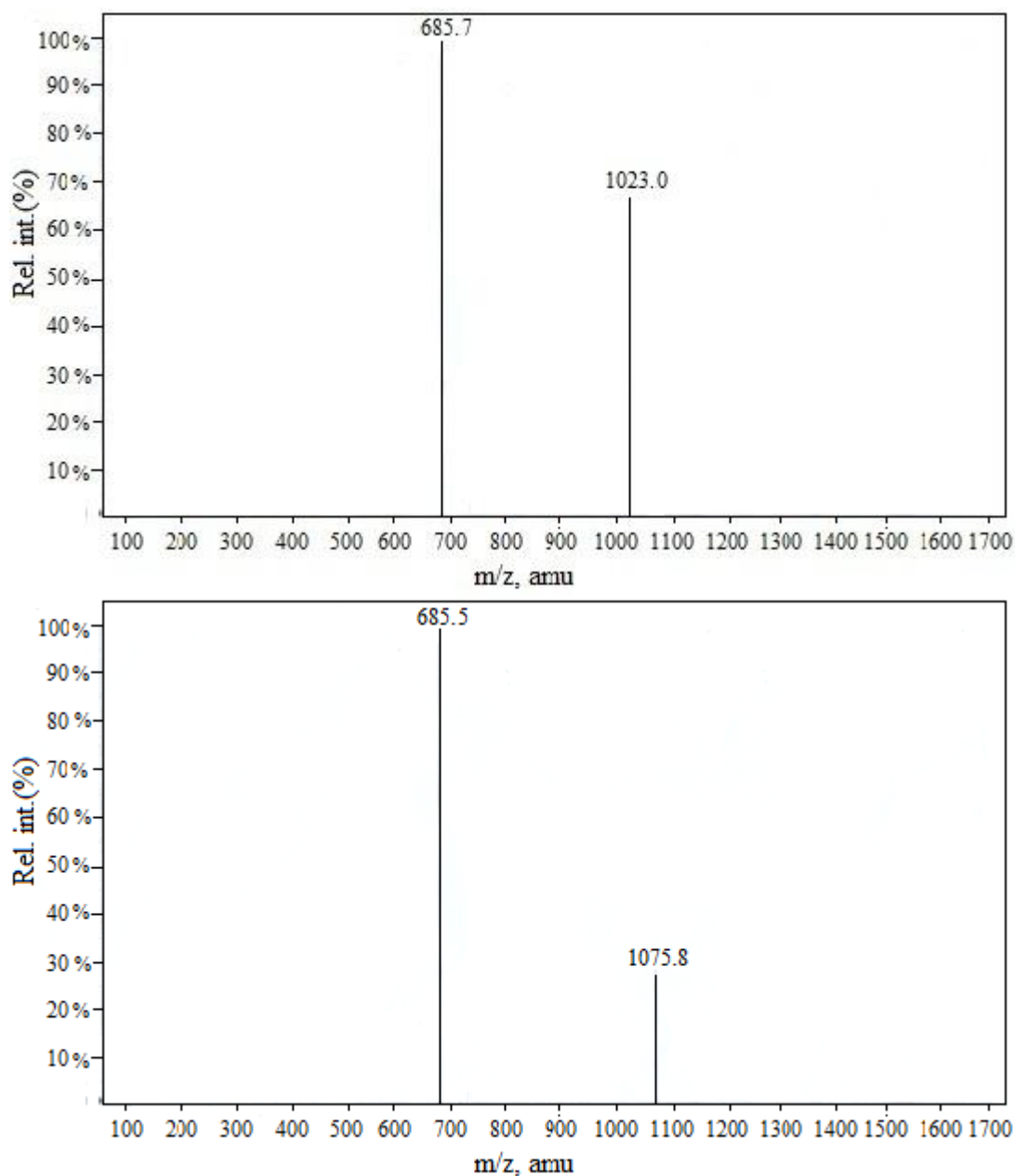
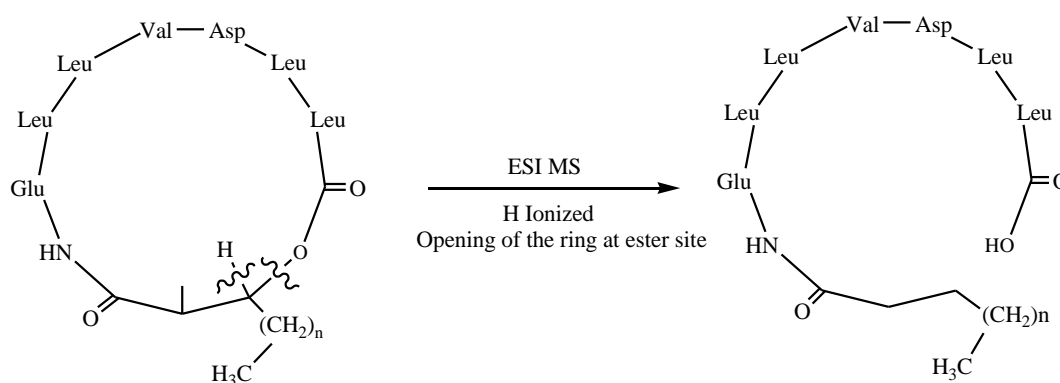


Fig. 4.21: ESI MS² showing the fragmentation of m/z 1023 and 1075.8

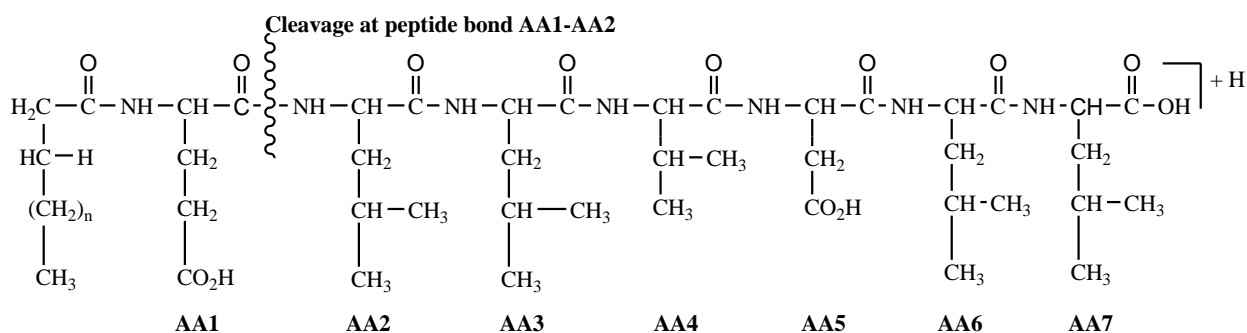
The disintegration of lipopeptide molecule is explained in detail in Fig 4.22b and 4.22c with the cleavage occurring in the lipopeptide molecule. Initially the fragmentation

occurred at the ester site opening the ring of lipopeptide molecule followed by the fragmentation between AA₁ and AA₂ releasing the peptide chain. The peak at m/z 685 in MS² spectra corresponds to peptide moiety from AA₂ to AA₇ in sequence of peptide chain including water due to binding of [H]⁺ and [OH]⁻ ions during the cleavage at the ester site in positive ion ESI-MS i.e. [(H)AA₂ - AA₇(OH) + H]⁺ = 685. AA₂ and AA₇ correspond to second and seventh amino acid respectively in the peptide sequence i.e. Glu-Leu-Leu-Val-Asp-Leu-Leu in the heptapeptide type of lipopeptide.

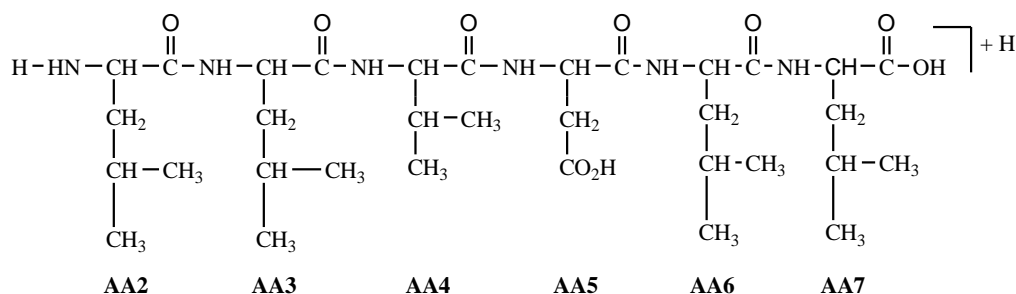
(a)



(b)



(c)



$$[(H) AA2\text{---}AA7 (OH)+H]^+ = m/z 685$$

Fig.4.22: Sequence of cleavage of surfactin molecule during ESI MS
(a) opening of the ester ring.(b) cleavage after ring opening
(c) fragment with m/z 685 with peptide sequence from AA₂ to AA₇

The peptide moiety after cleavage between AA₁ and AA₂ is expressed as [(H) AA₂ - AA₇(OH) + H]⁺ having molar mass = 685 and after removing the water molecule it has a mass of 685 - [H₂O] = 685-18 = 667, which is the molecular weight of the peptide sequence alone without considering the H₂O molecule. Further, the addition of AA₁ (glutamic acid having molar mass 128) to the molar mass of 667 results in a molar mass of 667+ 128 = 795, which now includes all the seven amino acids present in surfactin. Therefore, the value 795 is considered as the base and further the molecular weight is evaluated by addition of the aliphatic chain with peptide base of 795 which results in a total molar mass of 795 + [71+ (CH₂)_n], where [71+(CH₂)_n] is the weight calculated for the aliphatic chain and ‘n’ stands for methylene groups in the aliphatic chain as shown in Fig 4.15.

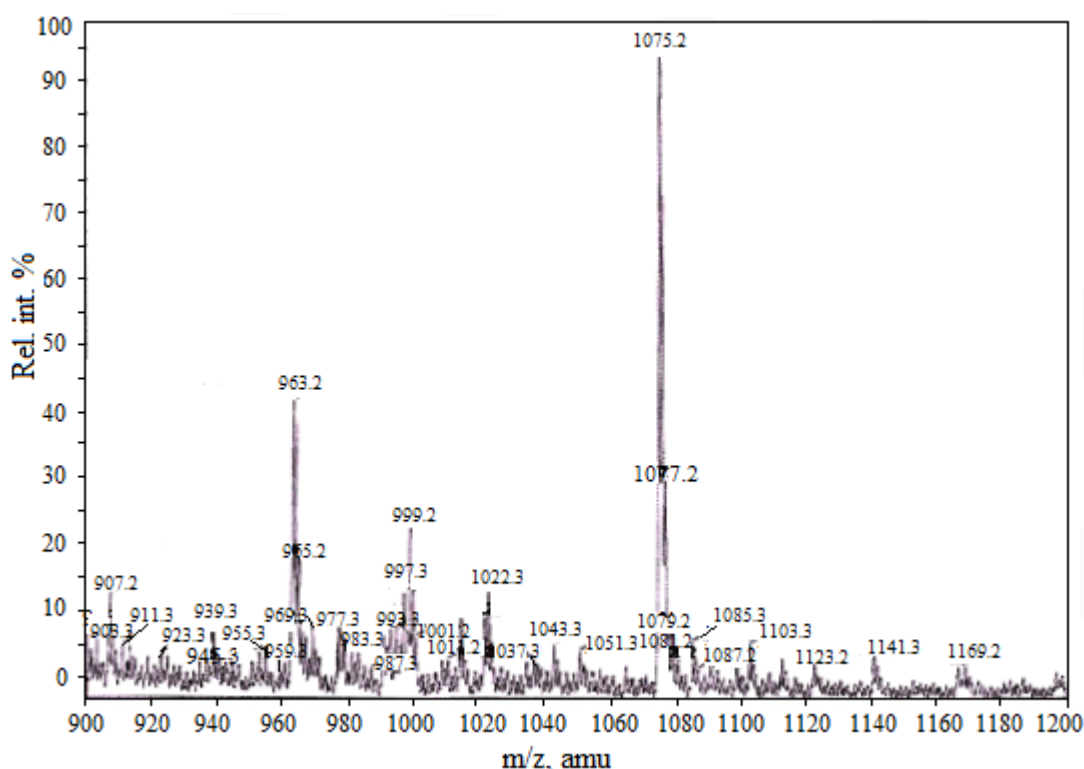


Fig 4.23: ESI-MS of the surfactin obtained from molasses showing [M+H]⁺ peaks

Hence, for methylene chain length n=9 the molar mass becomes M=992, corresponding M⁺ =993, n=10, M⁺=1007, n=11, M⁺=1022, n=12, M⁺=1036, n=13, M⁺=1050, n=14, M⁺=1064, n=15, M⁺=1076. These values correspond to the major peaks and some smaller peaks of the experimentally obtained ESI-MS spectra. This confirms the cleavage at the ester site and further cleavage between AA₁ and AA₂. These results indicate that the sample consists of cyclopeptide with varying number of methylene groups attached to the aliphatic chains i.e. presence of higher and lower homologs of

surfactin. Since both the homologs at m/z 1076 and 1023 show a similarity in the peptide component, it also confirms the similarity in the peptide moiety. Figure 4.23 shows the ESI-MS for surfactin obtained from molasses with m/z values almost similar as that observed for surfactin from rice bran with predominance of m/z at 1076.

A detailed characterization revealed that the synthesized product was surfactin and its isoforms with the carbon chain length varying from 13 to 19. In both surfactin samples obtained by fermentation of rice bran and molasses using *Bacillus subtilis* MTCC 2423 there is predominance of surfactin of molecular weight 1076, with carbon chain length 19. The lipopeptide type of biosurfactant - surfactin molecular weight ranges between 979 to 1091 Da (Horowitz and Griffin, 1991).

4.8 Dynamic light scattering studies of surfactin solutions.

Characterization of the biosurfactant synthesized by the fermentation of rice bran and molasses using *B. subtilis* in this study revealed that the product was surfactin and its isoforms. Surfactin is an acidic lipopeptide, its structure is characterized by a cyclic peptide loop bonded to a linear fatty acid chain. It is amphiphilic in nature and has remarkable surface activity. It can reduce the surface tension of water from 72 to 27 mN/m at concentration as low as 20 μ M.

Microcalorimetry studies on surfactin solutions by Han et al. (2008) attribute the critical micelle concentration of surfactin to be 38 μ M, which is much lower than other ionic surfactants indicating that surfactin has very strong self-assembly ability. Further, the surfactin molecule consists of seven amino acid units, higher surfactin concentration tends to provide more chances of interaction with other surfactin molecule via hydrogen bonds leading to the formation of β -sheet structure of micelle aggregates which is not observed with chemically synthesized normal surfactant. Neutron reflectivity and small angle neutron scattering studies on surfactin by Li et al. (2009) indicate that the structure of its micelle is core-shell type with the hydrocarbon chain and the four hydrophobic leucines forming the core of the micelle. The micellar shape and size of surfactin was observed to change with pH and addition of ions (Knoblich et al., 1995).

Dynamic light scattering (DLS) measurements using Malvern Nano ZS zetasizer at 90° angle at 25°C was used in this study to determine micelle size distribution of surfactin.

Surfactin was dissolved in 0.05 mol/L Tris buffer (tris amino methane in water) and the pH was adjusted to 8.5 by using 0.1 M HCL. The hydrodynamic radius distribution that is measure of the surfactin micelle size was determined at two different concentrations 38.3 μ M/L and 57.4 μ M/L i.e. at its CMC concentration and concentrations considerably higher than CMC values as shown in Figure 4.24 (a) and (b) respectively.

At solution concentration of 38.3 μ M/L the micelle size distribution is quite broad ranging from 25 to 500 nm, the intensity of the peak is \sim 10% and is attributed to the surfactin micelles and micelle aggregates in solution. Bimodal size distribution is observed at surfactin concentration of 57.4 μ M/L. One peak is in size range of 15-40 nm and the other at 139 nm, the width of this distribution 40 – 400nm. The size distribution is likely contributed by the various iso-forms of surfactin present in the solution as well as the shape of the micelle. The second peak having intensity of \sim 90% is attributed to aggregates of micelles formed by intermicelle hydrogen bonds. Li et al. (2008) have also reported bimodal distribution of micelles sizes by DLS measurement in surfactin solutions of 40 μ M/L concentration with peaks at \sim 100 nm and 500 nm sizes.

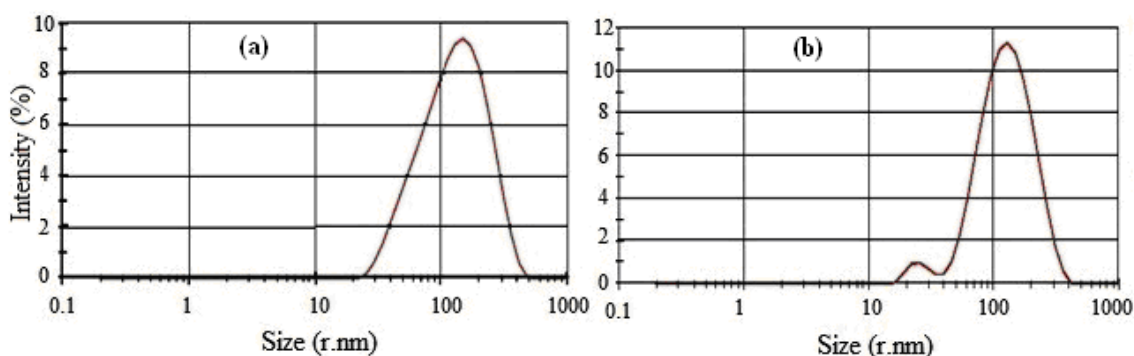


Fig. 4.24: Micelle size distribution of surfactin (a) Concentration 38.3 μ M/L, (b) concentration 57.4 μ M/L

It is known that the CMC value of surfactin decreases in the presence of counterions, the extent of change depends on the type of counterions and its concentration. There are two competing tendencies in the formation of micelles of ionic surfactants: removal of hydrocarbon chains from water favors aggregation, while the electrostatic repulsions between the ionic head groups oppose aggregation. Counterions stabilize ionic surfactant micelles by binding to the micelles and screening the electrostatic repulsions, therefore binding affinity of the counterions influences the process of micellization.

The effect of a univalent and a bivalent ion on surfactin micelle size distribution was studied. K^+ ions were added to 57.4 μ M/L surfactin solution prepared in Tris buffer such that it resulted in a solution of 0.1 M K^+ concentration. The results are presented in Figure 4.25. It shows two separate size distributions instead of a broad size distribution observed in Fig. 4.24a in the absence of counter ions. A low intensity distribution is observed between 40 nm and 90 nm while a high intensity distribution is observed between 300 nm and 750 nm. The lower size distribution is attributed to individual micelles while the higher size distribution is contributed by micelle aggregation. The cause for such distinct micelle size distributions in the presence of K^+ ions plausibly stems from the fact that addition of univalent cations leads to a decrease in surfactin CMC value making it is easier to form micelles at the same concentration and more fatty acid chains assemble in the micelle core creating an environment that favors aggregation.

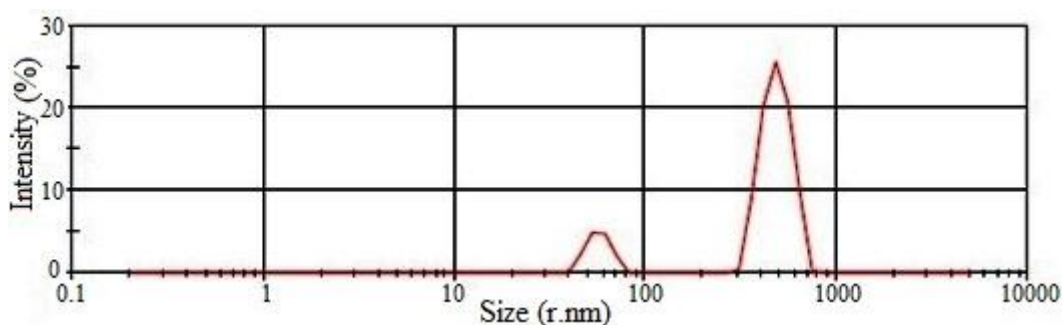


Fig.4.25: Effect of K^+ ions on micelle size distribution of surfactin.

Li et al. (2009) have shown that valence of counterions strongly affect surfactin micellization, with divalent ions reducing surfactin CMC value to a much greater extent than univalent ions such as and Li^+ . The peptide ring of surfactin forms a ‘horse saddle’ topology in aqueous solution with the two charged residues forming a ‘claw’ which binds the divalent cations. Thus, the divalent cations induce a tighter molecular packing and stronger structure of surfactin micelles. Osman et al. (1998) has shown that Ca^{2+} ions have special interaction with surfactin even at very low concentration compared with other divalent cations perhaps because the Ca^{2+} ion fits the surfactin structure and has strong chelation, greater than other divalent ions such as Mg^{2+} or Ba^{2+} .

Micelle size distribution was determined for surfactin solutions prepared in tris buffer having 57.4 μ M/L surfactin concentration in presence of Ca^{2+} counter ions of concentration 2×10^{-4} mol/L. Results shown in Fig 4.26 indicate the presence of two distributions as observed in the presence of the univalent K^+ ions, but the intensity and width of the primary size range is quite small between 25 and 50 nm while the second

distribution is also quite narrow between 200-400 nm but quite intense showing peak intensity of 38% at size of 300 nm.

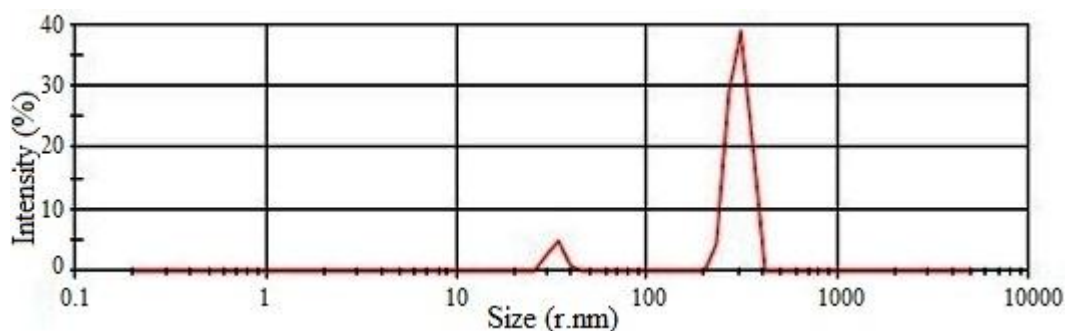


Fig.4.26: Effect of Ca^{2+} ions on micelle size distribution of surfactin.

The change in the size of micelle aggregates upon addition of counterions clearly indicates its effect on micelle size distribution. The ionic radius of potassium consisting of single positive charge is higher compared to the ionic radius of calcium with two positive charges. The surfactin molecule consists of two negative charges, therefore two potassium ions consisting single positive charge on each bind with a single surfactin molecule while a single calcium ion with two positive charges on each tend to bind and form a claw structure with one surfactin molecule. Therefore, the size of micelle aggregates available upon binding of two potassium ion on single surfactin molecule would be relatively larger compared to the binding of single calcium ion to one surfactin molecule. Ionic radius as well as the number of charges available on ions had its effect on the formation of larger micelle aggregates.

4.9 Scale- up and production economics

4.9.1 Scale up

Scale up of surfactin production from 200 ml sample size to 1000 ml sample size was attempted under identical conditions with similar standard operating procedures using rice bran (2%,w/v) as substrate with *B.subtilis* MTCC 2423 strain (2 % v/v).

Table 4.8 indicates a substantial increase in the yields of surfactin by a fivefold increase in sample volume from 200 ml to 1000ml. In absence of a pilot scale run, we can consider yields of surfactin obtained for the larger volume as the representative of the yield of surfactin likely to be obtained in its industrial production from rice bran by submerged fermentation using *B.subtilis* MTCC 2423. The surfactin yield was determined after three stage foam fractionation followed by acid precipitation. The

precipitates obtained were allowed to dry in an oven below 70°C and then weighed. The yield obtained on scale up was 6.02 g/kg rice bran in comparison 4.3 g/kg that was obtained during fermentation carried out with working volume of 200 ml which indicates about 1.4 times higher yield.

Table 4.8: Effect of scale up on the total yield of surfactin obtained from rice bran

Volume of Sample (ml)	Volume of foamate (ml)	Volume of residue (ml)	Recovery of Surfactin		Total Yield
			Foamate (mg)	Residue (mg)	
1000	263	737	83.5	36.4	6.0 g/kg rice bran
200	50	150	11.94	5.26	4.3 g/kg rice bran

The process development and economics is worked out based on the data generated in this work. One can consider that almost 70% surfactin can be recovered which is in line with the recoveries reported by investigators using membrane separation techniques (Sen and Swaminathan, 2005). However, some other investigators have reported recoveries to the tune of 90% (Ramnani et al., 2005) which appears to be difficult to achieve. There is always a possibility of enhancing the recovery by combination techniques using foam fractionation and membrane separation of the residue. However, one has to keep in mind that recovery is low if initial feed concentration to membrane separation unit is very dilute.

One has to balance the improvement in yields with the cost of energy required for processing. It is difficult to comment on the advantages of such combination techniques without appropriate data and optimizing the various parameters associated with it. Therefore, the preliminary costing of the process is completely worked on the data generated in this investigation using foam fractionation as the downstream processing technique.

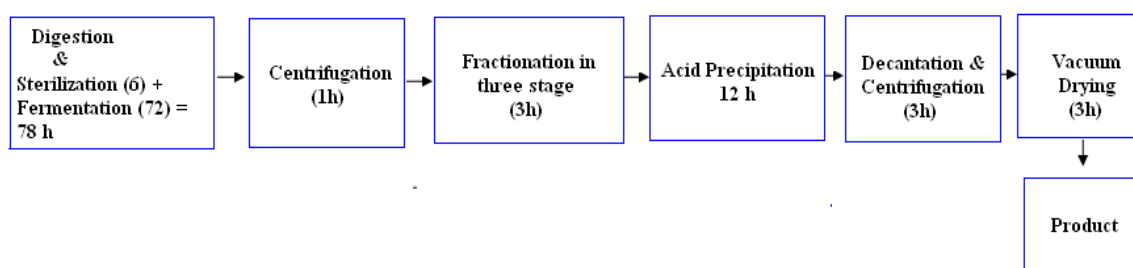


Fig.4.27: Process flow diagram of surfactin production and recovery

The process flow diagram of the surfactin production and recovery using rice bran as the substrate is shown in Figure 4.27, the tentative time required for the various steps of the process are listed in Table 4.9. A Gantt chart in the overlapping mode considering one batch of product every day is shown in Figure 4.28. The total time span turns out to be 100 hour for a batch irrespective of its size, the fermentation time is the dominant factor that dictates the overall production and scheduling scheme.

Table 4.9: Tentative time required in process steps

Process Steps	Time required(hours)
Sterilization and Digestion	6
Fermentation	72
Centrifugation	1
Foam Fractionation	3
Acid Precipitation	12
Decantation and Centrifugation	3
Vacuum Drying (Below 60°C)	3
Total Time	100

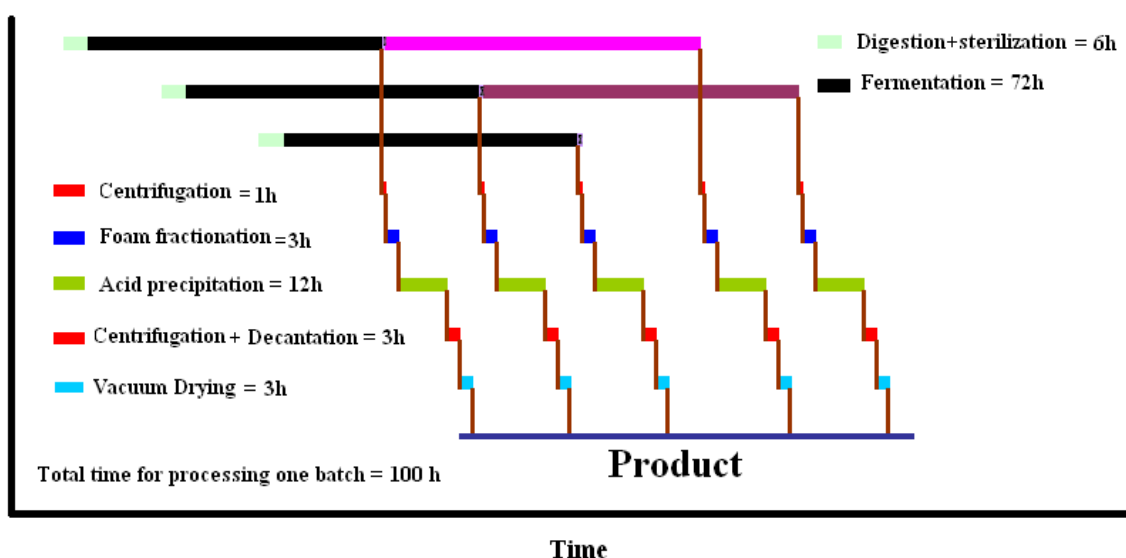


Fig.4.28: Overlapping Gantt chart for surfactin production

There is no data available regarding the commercial demand of surfactin but information available regarding its cost reveals that it is an extremely high value product (Sigma) therefore it is foreseen that the demand will be less and the market for surfactin will have to be built. In view of this, without resorting to any optimization of cost functions, a

rather modest capacity of 20 kg per annum was taken as the basis of working out the overall economics of the project as reported in Appendix 3.

4.9.2 Production Economics

The cost estimation for the production of biosurfactant – surfactin has been done with the basis of 20 kg of surfactin production per year. Rice bran is the major raw material utilized for fermentation and subsequent biosurfactant production which is procured from the nearby local rice mill. The cost estimation is done considering Bharuch and Ankleshwar region as the main site for production. The power is obtained from government electricity supply and a diesel generator set is maintained to restore power supply immediately during power cut.

The selection of equipments for the process are based on judicious consideration with the objective to keep the batch sizes small to facilitate media sterilization and downstream separations as well as to keep the production line intact in case some infection seeps in the fermentation set up. Based on the production capacity, with 2% substrate loading, the batch size to be handled per day will be 800 L. Further, considering that only two third loading of fluid is maintained in each fermentor to account for free space required because of liquid splash due to agitation etc, the volume of each fermentor turns out to be 1200 L. However, this volume is further split into four smaller units each of size 300 L with working volume of 200 L for the considerations listed above.

These fermentors can be accommodated in a single rack as is often the case in pharmaceutical sectors. Splitting the batch volume into smaller segments certainly contributes to fixed capital cost but introduces immense flexibility in the system that guards the process line against plausible failures that are not uncommon in fermentation processes.

The detailed cost estimation is worked out in Appendix 4. The direct cost and the indirect cost turn out to be Rs. 31,79,12,756.3 and Rs.7,07,80,138.13 respectively. The market selling price when fixed at Rs 20 per mg the payout period turns out to be ~2 years.

4.10 Summary

Biosurfactant production was done utilizing microbial culture *B.subtilis* MTCC 2423 with three different agricultural waste as substrates i.e. potato industry effluent, rice bran and molasses. A unique three stage foam fractionation technique was utilized for the recovery of biosurfactant from the fermented broth. The screening test i.e. drop collapse test was carried out to confirm the production of biosurfactant alongwith other test like surface tension reduction and further characterization of the product obtained was carried out to establish its identity. Alongwith biosurfactant monitoring, the growth of bacteria was also monitored by test like measurement of CFU, growth curve and total sugar curve. The surface tension of diluted samples was also measured i.e. critical micelle dilution (CMD) in order to get the idea of CMC.

The characterization test like FTIR was done to establish the presence of the functional groups in the biosurfactant sample and it revealed a lipopeptide type of biosurfactant with the presence of lactone carbonyl ring and amide groups. HPLC test was carried out and the curve obtained was compared with that of standard surfactin curve where there were many similarities in the retention peaks indicating that the lipopeptide type of biosurfactant was surfactin. TLC was carried to do preliminary characterization where the product gave spot with iodine vapors and spot was visible in UV test as well confirming the lipopeptide type of biosurfactant. The retention factor R_f value obtained was 0.525 and it closely match with that of surfactin reported earlier by other researchers.. The NMR test carried out revealed the presence of amide and other peaks relevant to that of surfactin type of lipopeptide. ESI-MS technique was utilized to get an idea about the molecular weight of lipopeptide type of biosurfactant. The test revealed the dominance of biosurfactant with molecular weight of 1076 da and the secondary MS^2 of the product ion revealed the presence of heptapeptide sequence of amino acids alongwith lipid chain of methylene groups. Thereby the ESI-MS confirmed that the product obtained was surfactin with higher molecular weight due to long fatty acid chain length.